

Review

Exploring Spin-Crossover Cobalt(II) Single-Ion Magnets as Multifunctional and Multiresponsive Magnetic Devices: Advancements and Prospects in Molecular Spintronics and Quantum Computing Technologies [†]

Renato Rabelo ^{1,2}, Luminita M. Toma ¹, Abdeslem Bentama ³, Salah-Eddine Stiriba ¹ , Rafael Ruiz-García ¹ and Joan Cano ^{1,*} 

¹ Instituto de Ciencia Molecular (ICMol), Universitat de València, 46980 Paterna, València, Spain; renato_rabelo@ufg.br (R.R.); lumimtoma@gmail.com (L.M.T.); salah.stiriba@uv.es (S.-E.S.); rafael.ruiz@uv.es (R.R.-G.)

² Instituto de Química, Universidade Federal de Goiás, Goiânia 74690-900, Brazil

³ Laboratoire de Chimie Organique Appliquée, Faculté des Sciences Techniques de Fès, Université Sidi Mohammed Ben Abdellah, Fès 30000, Morocco; abdeslem.bentama@usmba.ac.ma

* Correspondence: joan.cano@uv.es

[†] Dedicated to Professors Miguel Julve and Francesc Lloret, two outstanding chemists, excellent teachers, best friends, and colleagues on the occasion of their retirement and, particularly, to the memory of Miguel Julve, who passed away in July 2024.

Abstract: Spin-crossover (SCO) and single-ion magnets (SIMs), or their mixed SCO-SIM derivatives, are a convenient solution in the evolution from molecular magnetism toward molecular spintronics and quantum computing. Herein, we report on the current trends and future directions on the use of mononuclear six-coordinate Co^{II} SCO-SIM complexes with potential opto-, electro-, or chemo-active 2,6-pyridinediimine (PDI)- and 2,2':6',2'-terpyridine (TERPY)-type ligands as archetypical examples of multifunctional and multiresponsive magnetic devices for applications in molecular spintronics and quantum computing technologies. This unique class of spin-crossover cobalt(II) molecular nanomagnets is particularly well suited for addressing and scaling on different supports, like metal molecular junctions or carbon nanomaterials (CNMs) and metal–organic frameworks (MOFs) or metal-covalent organic frameworks (MCOFs), in order to measure the single-molecule electron transport and quantum coherence properties, which are two major challenges in single-molecule spintronics (SMS) and quantum information processing (QIP).

Keywords: cobalt complexes; coordination chemistry; dynamic molecular systems; ligand design; non-innocent ligands; single-ion magnets; spin-crossover; molecular magnetism; molecular spintronics; quantum computing



Citation: Rabelo, R.; Toma, L.M.; Bentama, A.; Stiriba, S.-E.; Ruiz-García, R.; Cano, J. Exploring Spin-Crossover Cobalt(II) Single-Ion Magnets as Multifunctional and Multiresponsive Magnetic Devices: Advancements and Prospects in Molecular Spintronics and Quantum Computing Technologies.

Magnetochemistry **2024**, *10*, 107.

<https://doi.org/10.3390/magnetochemistry10120107>

Academic Editor: Talal Mallah

Received: 9 November 2024

Revised: 9 December 2024

Accepted: 13 December 2024

Published: 17 December 2024



Copyright: © 2024 by the authors. Licensee MDPI, Basel, Switzerland. This article is an open access article distributed under the terms and conditions of the Creative Commons Attribution (CC BY) license (<https://creativecommons.org/licenses/by/4.0/>).

1. Introduction and Background

Faster, smaller, cheaper—this has been the trend in computing for the last decades. Since 1947, electronics and computing have experienced a booming revolution with the invention of the primary examples of working transistors based on germanium and silicon materials and their subsequent developments as integrated systems. These technologies guided us to what is now known as the digital revolution. Unfortunately, one of the established bases of the digital revolution—Intel co-founder Gordon Moore’s prediction that the density of transistors in integrated systems would be doubled every two years, known as the Moore’s Law [1]—is nearing its end. In 1959, the physicist and Nobel prize winner Richard Feynman and his iconic phrase, “There’s plenty of room at the bottom”, granted thoughtful insights into and warmed up the nanotechnology and nanoscience fields [2]. Feynman’s forward-thinking ideas suggested that nanotechnology could enable

a proper toolkit to take the miniaturization to atom scale, offering a pathway to enhance system functionality and overcome current limitations.

Spintronics is a promising way to miniaturize electronic circuits, but also a more efficient technology that might replace the current device, the complementary metal-oxide-semiconductor (CMOS), by leading to highly integrated systems. This novel approach relies on the use of spin (and, thus, its associated magnetic moment) instead of only the electrical charge for device functionality. The electron spin is already being applied in computing to read data in hard disk drives based on the giant magnetoresistance (GMR) effect, discovered by Nobel Prize winners Albert Fert and Peter Grunberg [3,4]. Nevertheless, beyond that, once the electron spin is a two-level system, it is an inherent candidate for realizing a quantum bit (qubit) in quantum information processing (QIP) [5].

A variety of qubit-based algorithms have been developed since the 1990s. A priori, these algorithms can handle very complex calculations that are not available in current classical computers. In 2019, IBM unveiled the first quantum computer designed for commercial use, the IBM Q System One, which operates with twenty qubits. Recently, Google claimed the achievement of quantum supremacy with its 54-qubit Sycamore processor, which could perform, in two-hundred seconds, a calculation that would have taken ten thousand years to the most powerful non-quantum computer [6]. Unlike the IBM Q System One and Google's Sycamore systems that use superconducting qubits, other proposals for a quantum computer emerged using photons, named Jiuzhang, which generates up to 76 output photons and allows for the quantum cloning of two-phonon entangled states for the first time [7,8].

As the race toward quantum supremacy intensifies and electronics nears the limits of silicon, the development and implementation of spintronic components are becoming increasingly crucial. These technologies promise enhanced information processing performance and higher-density storage at lower costs, following the familiar trend of faster, smaller, and cheaper devices [9,10]. To date, spintronic devices have relied on conventional materials like inorganic metals and semiconductors. However, the prospect of a spin-based quantum computing machine is no longer far-fetched [11–13].

A new field, known as single-molecule spintronics (SMS), has emerged, combining spintronic concepts with the unique quantum properties of molecular systems at the nanoscale [14–29]. SMS offers several key advantages:

- (i) It provides an ideal platform for studying and understanding the fundamental principles of spintronics;
- (ii) It enables the creation of devices governed by quantum mechanics;
- (iii) It achieves the ultimate level of miniaturization for spintronic devices;
- (iv) It leverages a broad range of chemical tools to optimize quantum properties for various device architectures and applications, and, most importantly;
- (v) It paves the way for retrieving information from dynamic devices integrated into computers or sensors, facilitating a clear and efficient information read-out process.

Mononuclear spin-crossover (SCO) [30–47] and single-molecule magnet (SMM) compounds, also known as single-ion magnets (SIMs) [48–60], represent the smallest magnetic units in molecular magnetism (MM). Due to their dynamic molecular and quantum behavior, these compounds have promising applications in quantum computing and high-density information storage. Their multifunctional, multiresponsive, and bistable properties, along with their nanoscale size, ease of manipulation, and versatile addressing options, make SCO and SIM compounds ideal synthetic and theoretical models for fundamental studies on the phenomena that rule SMS and QIP [61–73]. Indeed, both classes of molecules are strong candidates for active components in molecular spintronic circuits and quantum computers.

1.1. SCO Complexes as Spin Quantum Nanodevices in SMS

Using a single molecule as a spin carrier represents the ultimate level of miniaturization for an SMS device. SCO molecules have garnered attention due to their ability to respond to multiple stimuli, making them well suited as conductive elements within nanoscale structures, known as molecular junctions. The most basic device configuration consists of a source and

drain electrode to establish electron flux. A more complex setup, the transistor, incorporates an additional gate electrode to regulate electron flow through the molecule by applying a potential. Notably, integrating SCO molecules into these devices has yielded promising results.

In an experiment conducted by Park et al., thiol-functionalized terpyridine-cobalt(II) complexes with the formula $[\text{Co}(\text{TERPY}\{\text{CH}_2\}_n\text{SH})_2]^{2+}$, where $n = 0$ or 5 , molecules that are part of the well-known family of octahedral spin-crossover (SCO) cobalt(II) imine complexes [35] connect two gold electrodes [61]. The study demonstrated that altering the number of methylene groups in the ligand could control electron transport properties. When the low-spin (LS) cobalt(II) complex ($S = 1/2$) with the short linker ($n = 0$) was anchored to the gold electrodes, a Kondo peak appeared, evincing a strong coupling regime. In contrast, using a longer carbon chain ($n = 5$) as the linker resulted in weak coupling, where the Coulomb blockade dominated the behavior. Subsequently, the parent $[\text{Co}(\text{TERPY-SH})_2]^{2+}$ complex was connected to two mobile gold electrodes [62]. The mechanical manipulation of the junction enabled spin control by altering molecular symmetry, leading to the splitting of the Kondo peak as the molecule was stretched.

The authors concluded that the observed Kondo resonance arises from a triplet spin ground state originating from the reduction in the metal to a high-spin (HS) cobalt(I) complex ($S = 1$) as the current flows through the molecule and not the molecular changes linked to the HS/LS transition on the original cobalt(II) complex, as previously seen in related iron(II) SCO complexes with redox-active ligands such as 2,6-bis(pyrazol-1-yl)pyridine (DPZPY) and 3,5-bis(pyrazol-1-yl)-4,4'-bipyridine (DPZBPY) [63]. In the last case, the authors suggested that the observed Kondo peak splitting, as a function of gate voltage, was due to changes in the charge of the two ancillary ligands, modifying the spin state but not the metal oxidation state, as supported by theoretical calculations on the $[\text{Fe}(\text{DPZPY})_2]^{2+}$ model complex [63]. This charge-induced spin-crossover was associated with the transformation of the LS iron(II) ($S = 0$) complex into the antiferromagnetically coupled, doubly reduced π -radical anion HS iron(II) ($S = 2$) species, $[\text{Fe}^{\text{II}}(\text{DPZBPY}^{\bullet-})_2]$, with a resulting $S = 1$ state.

Harzman et al. reported another innovative method for controlling electron transport in single-molecule spintronic devices, as illustrated in Figure 1 [64]. The novelty lies in the sensitivity of the spin state to the spatial arrangement of the ligands and the overall distortion of the asymmetric $[\text{Fe}(\text{TERPY-PhSAC})(\text{TERPY-PhXY})]^{2+}$ complex (Figure 1a), where two sulfur-containing groups modify one TERPY-PhSAC ligand to allow the complex to be anchoring to the surface of gold electrodes, while the other TERPY-PhXY ligand containing two polar groups remains free to rotate. The strong ligand field pairs the electrons, resulting in a diamagnetic LS ground state for the iron(II) complex in its almost ideal geometry (Figure 1b, top). However, mechanical distortion of the coordination environment reduces symmetry and weakens the ligand field, making e_g orbitals accessible, which results in a paramagnetic HS ground state (Figure 1b, bottom). The application of an electric field polarizes the free TERPY ligand, causing a reduction on the symmetry of the octahedral coordination sphere, which alters the conductance across the junction as a bias-dependent spin-switching mechanism of control. In contrast, when the SCO iron(II) $[\text{Fe}(\text{S-BPP})_2](\text{ClO}_4)_2$ complex [S-BPP = (S)-(4-{[2,6-(dipyrazol-1-yl)pyrid-4-yl]ethynyl}phenyl)ethanethioate] was integrated into gold nanoparticle arrays, the resistance exhibited a minimum around 200 K, according to a higher molecular resistance of the HS state [65].

Remarkable results were also achieved by addressing the individual *trans*-bis(thiocyanate) iron(II) SCO molecules $[\text{FeL}_2(\text{NCS})_2]$ {L = 3-(2-pyridyl)[1-3]triazolo [1,5-a]pyridine (TZPY) and *N,N'*-bis(1-pyridin-2-ylethylidene)-2,2-dimethylpropane-1,3-diamine (BEPYDMP)} between a gold surface and the ferromagnetic nickel tip of the scanning tunneling microscope (STM), as depicted in Figure 2 [67,69]. In their seminal work, Aragonès et al. found out that, when subjected to a spin-polarized current, the device exhibited spin state-dependent electron transport, in which the TZPY ligand acts like a spin filter, and the HS complex increases the single-molecule conductance as the polarization of the nickel electrode shifted from spin-up (α) to spin-down (β) [69]. In contrast, the electrical conductance remained

unchanged when the diamagnetic LS iron(II) complex with the BEPYDMP ligand was concerned [67]. These results agreed with earlier theoretical predictions by Aravena and Ruiz, who anticipated higher conductance for the aforementioned paramagnetic HS iron(II) complex with the TZPY ligand [66].

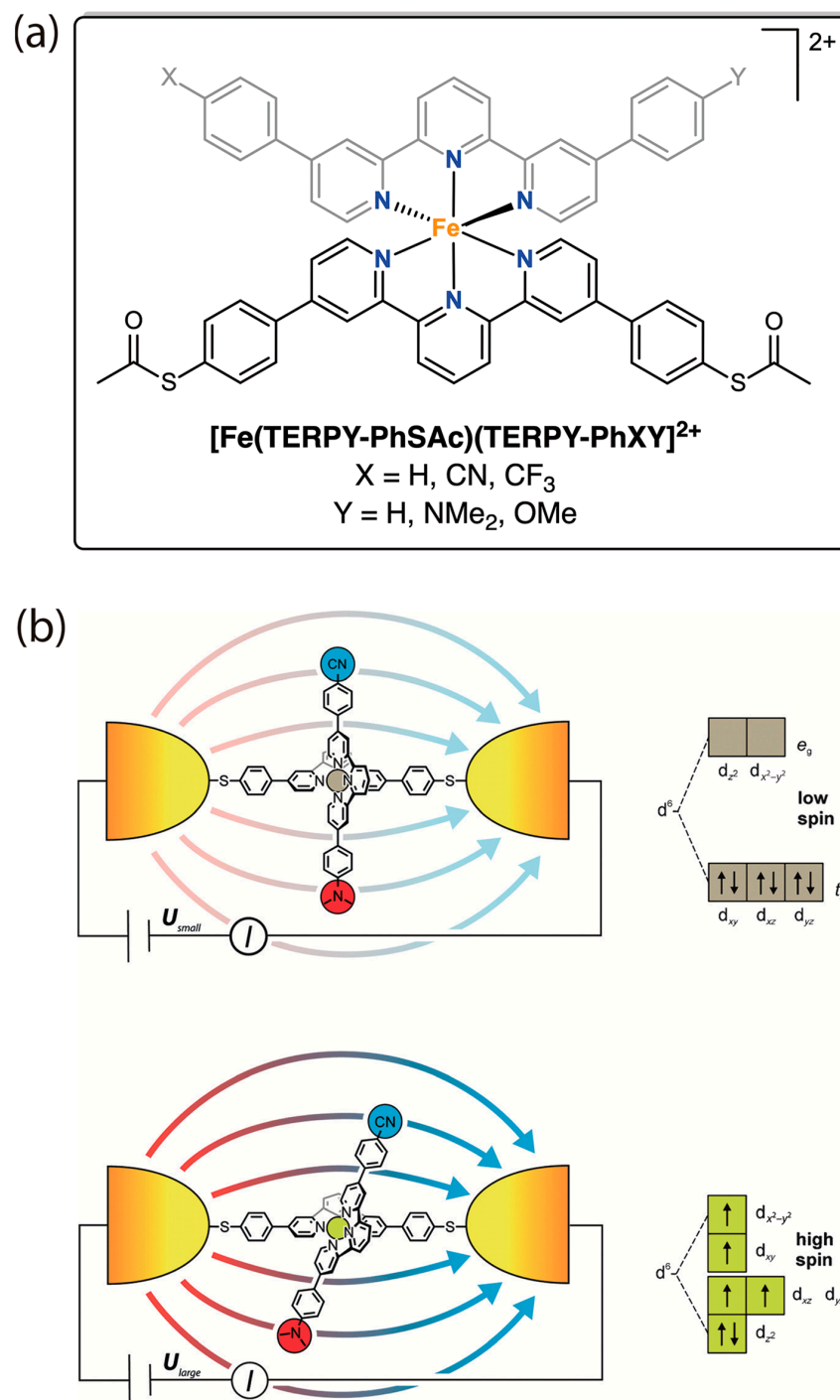


Figure 1. (a) The general chemical structure of the series of polar heteroleptic iron(II) complexes of formula $[\text{Fe}(\text{TERPY-PhSAc})(\text{TERPY-PhXY})]^{2+}$ as a prototype of the electric field-effect spin quantum transistor. (b) An illustration of the single-molecule junction constructed from the iron(II) complex connecting two gold electrodes at a small, applied voltage (top) and the distorted HS complex due to the alignment of the ligand TERPY-PhCN(NMe₂) to the applied electric field. Adapted with permission from Ref. [64].

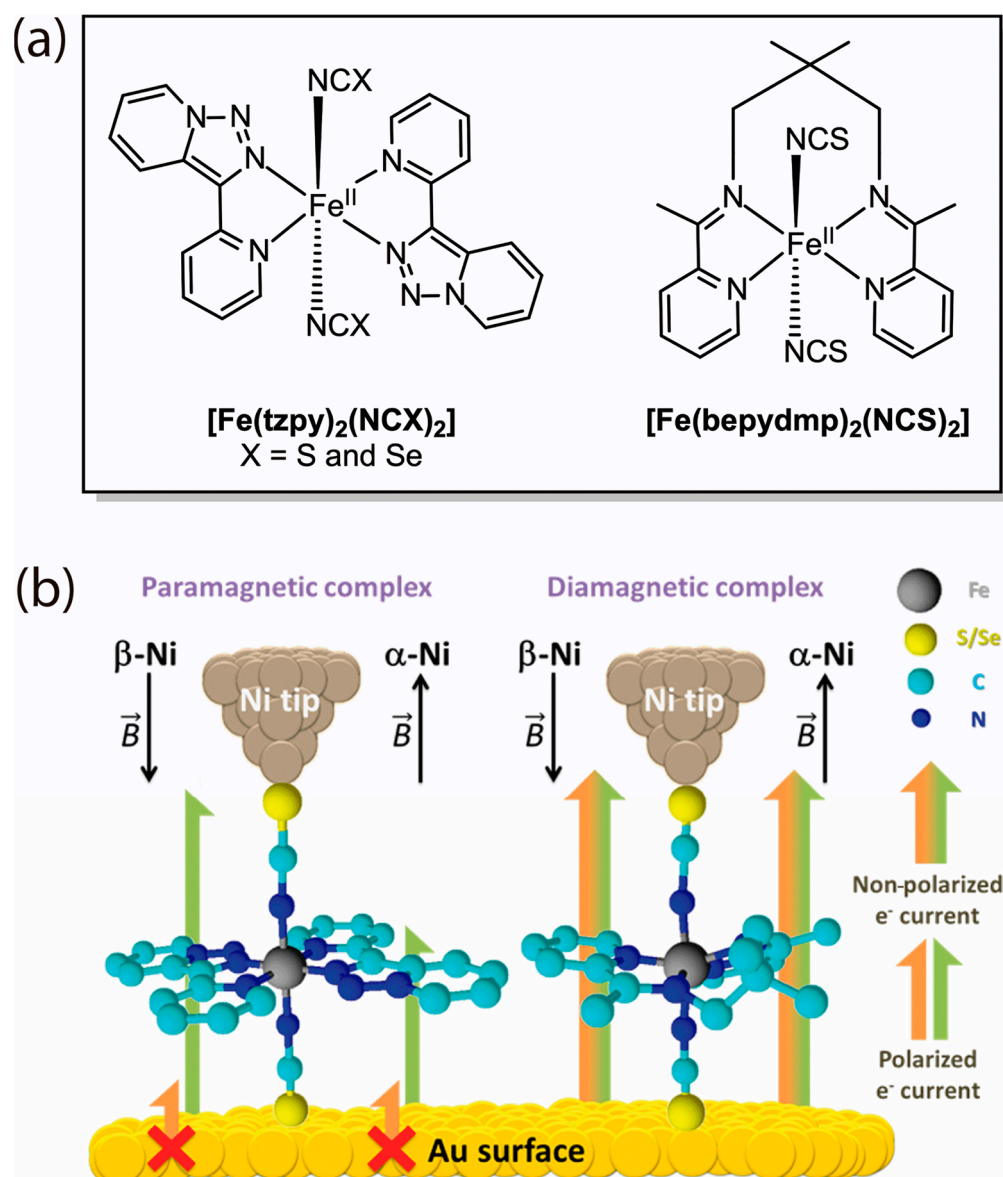


Figure 2. (a) General chemical structures of the mononuclear iron(II) complexes [Fe(TZPY)₂(NCX)₂] (X = S and Se) and [Fe(BEPYDMP)₂(NCS)₂] as a prototype of the spin quantum filter. (b) An illustration of the conductance switching of the spin-dependent electron transport in a real single-molecule junction constructed from [Fe(TZPY)₂(NCX)₂] (X = S and Se) and [Fe(BEPYDMP)₂(NCS)₂] connected between the gold surface and the ferromagnetic nickel tip of the STM with opposite spin polarizations. Adapted with permission from Ref. [67].

Graphene is an attractive component for hybrid device materials due to its exceptional surface sensitivity to environmental dielectric properties [68]. In this context, the electrical read-out of light-induced spin transition was investigated by building a thin film of the SCO iron(II) complex [Fe(HBDMPZ)₂] [HBDMPZ = hydrotris(3-5-dimethylpyrazole)borate] on a graphene sensing layer. The switch from diamagnetic LS to paramagnetic HS increased the conductance of the graphene channel under both light irradiation and temperature stimulus [69]. These findings highlight the critical role of single molecules in addressing the search for new functionalities that would give rise to future nanoscale spintronic devices.

1.2. SIMs as Spin Quantum Nanodevices in SMS

Organic molecules have been extensively used in the design of promising electronic devices, leading to important advancements in applications such as semiconductors, light-emitting diodes (LEDs), photovoltaic cells, spin valves, and field-effect transistors (FETs) [70]. Since the discovery of GMR in purely inorganic materials, the study of electron transport, combined with magnetic properties associated with the electron spin, has pushed molecular electronics into a newly emerging area with vast possibilities: molecular spintronics. Some examples of spintronic uses of SIMs as quantum spin transistors and spin valves are detailed hereunder.

An outstanding example of a spintronic transistor is the oxidized double-decker [Tb(PC)₂] SIM molecule (PC = phthalocyanine) absorbed on a gold surface, as shown in Figure 3 [71]. This device exhibits a Kondo resonance peak in electrical conductance at zero-bias voltage ($V = 0$), which indicates transistor-like behavior. This Kondo effect arises from the unpaired spin on a π -orbital of the oxidized PC ligand since the large magnetic anisotropy of the Tb^{III} ion prevents the degeneration of states necessary to produce Kondo signals. Moreover, controlled current pulses can significantly alter the conformation of the SIM, rotating the upper PC ligand of [Tb(PC)₂] from the ideal azimuthal angle (θ) of 45° to 30° (Figure 3a). This conformational change reversibly commutes the spin, switching the Kondo state ON and OFF (Figure 3b).

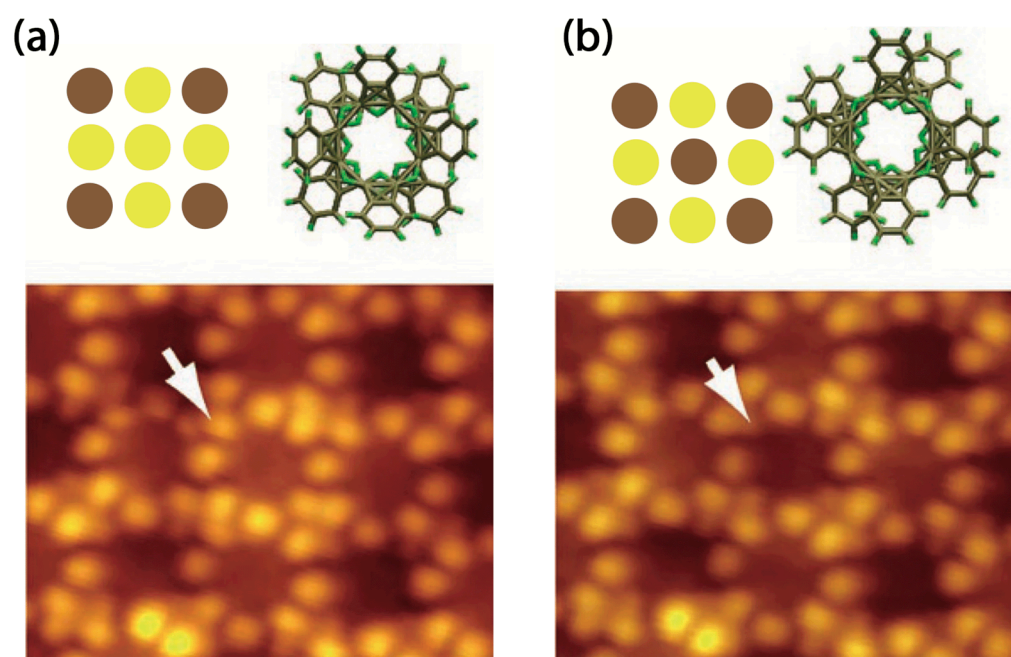


Figure 3. STM images of the conversion of the mononuclear terbium(III) complex [Tb(PC)₂] from $\theta = 45^\circ$ (a) to $\theta = 30^\circ$ (b) by applying a current pulse as a prototype of the spin quantum transistor. An arrow marks the target molecule, and magnified images are shown in the bottom panel. Changes in the contrast and the top view of the center molecule are schematically illustrated. Adapted with permission from Ref. [71].

Taking advantage of the GMR, spin valves, a key component of modern hard drives, offer another possible solution for memory device implementation. Traditionally, these devices utilize metal layers. However, recent research has explored a novel design incorporating SIMs or their supramolecular arrays coupled to a single-walled carbon nanotube (SWCNT), as illustrated in Figure 4 [72,73]. The chosen SIM was the mononuclear terbium(III) derivative [Tb(PC)(Hx₆BuOpyrPC)] accounting for one modified pyrene and six hexyl groups into one of the two PC rings, serving as anchoring points (Figure 4a). Notably, both the energy barrier and relaxation time increased upon anchoring, likely due to sup-

pressing the intermolecular interactions between the SIM units [72]. The device consists of a source and drain connected by an SWCNT, to which the SIM randomly binds through supramolecular interactions (Figure 4b) [73]. The hypothesis was that the giant magnetic anisotropy of the SIM could affect electron transport through the SWCNT. Experimental results confirmed that, when a magnetic field is applied in the plane of the device and then reversed, magnetoresistance ratios rise to 300% at temperatures below 1 K. A simplified model suggests that two SIM molecules (A and B) in the channel generate an effective energy barrier when their spin moments are antiparallel, an effective energy barrier forms, hindering charge flow (Figure 4b, top); however, if the spin moment of B switches under the magnetic field, high conductance is restored across the SWCNT (Figure 4b, bottom).

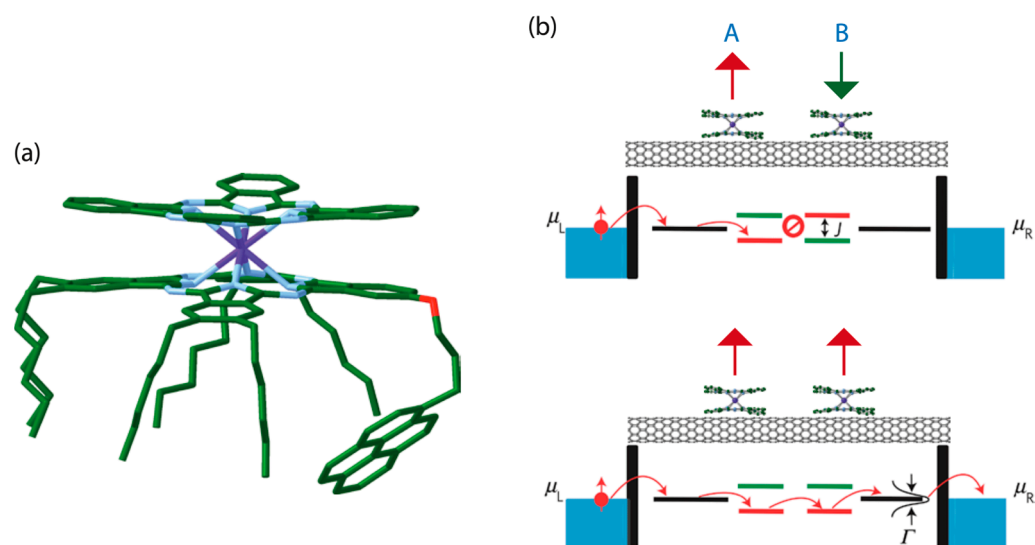


Figure 4. (a) The chemical structure of the mononuclear terbium(III) complex [Tb(PC)(Hx₆BuOpyr PC)] as a prototype of the spin quantum valve. (b) An illustration of the magnetoresistance switching mechanism for an SWCNT with two anchored 4f SIMs. The thick red and green arrows are the localized spins of the 4f SIMs, while the thin red arrows represent the spin-polarized conduction electrons across the SWCNT. Adapted with permission from Ref. [73].

2. Current Trends and Future Directions

A wide array of SCO systems based on mononuclear iron(II) and cobalt(II) complexes is well known and has served as an essential platform for understanding the SCO phenomenon [34,35,74–87]. Meanwhile, cobalt(II) SIMs have garnered significant attention due to the inherent high magnetic anisotropy of the HS Co^{II} ion and its extensive coordination chemistry [81,88–96]. However, the coexistence of both bistabilities—SCO and SIMs—in a single system remains rare. In first-row transition metal complexes, SIM behavior typically manifests only at very low temperatures, while thermally induced HS/LS transitions occur at higher temperatures, resulting in a diamagnetic or paramagnetic LS state ($S = 0$ or $1/2$ for Fe^{II} and Co^{II} ions) at low temperatures. To date, only a few studies report the coexistence of SCO and SIM behavior in cobalt(II)-based systems [97–108]. This coexistence is not possible for the Fe^{II} ion with a diamagnetic LS state, but it could happen in the HS state. Thus, only three known SCO-SIM systems have been observed in metastable, magnetically anisotropic HS excited states ($S^* = 2$), achieved through light irradiation via a light-induced excited spin-state trapping (LIESST) process [109–111].

Multifunctional and multiresponsive cobalt(II)-based SCO-SIMs have gained renewed interest in the ongoing transition from MM to SMS and QIP [112]. The cornerstone of this advancement lies in designing and synthesizing novel classes of potentially opto-, electro-, and chemo-active ligands and, therefore, capable of allowing precise control and switching of the spin transition and magnetic relaxation dynamics on metal centers.

2.1. Co^{II} SCO-SIMs as Spin Quantum Nanodevices in SMS and QIP

As we continue going further on the road from MM to SMS, our journey has led us to some new insightful outcomes that we will share and discuss below since they will undoubtedly help to reinforce the consolidated MM field while also offering alternative pathways in the emerging SMS domain. Hence, because of their unusual combination of chemical (redox and Brønsted or Lewis acidity) and physical (magnetic and optical or luminescent) properties arising from metal and ligand components, Co^{II}-PDI and Co^{II}-TERPY complexes are well suited for the design of multifunctional, multiresponsive advanced magnetic materials for SMS nanotechnology. In particular, they emerge as promising candidates for spintronic nanodevices, like spin quantum capacitors and switches.

2.1.1. Molecular Spin Quantum Capacitors and Supercapacitors

Transition metal complexes containing non-innocent electroactive ligands have been extensively studied as single-molecule spintronic devices for charge storage applications [113–115]. The ability to access multiple ligand-based electron reductions (up to four) and one metal-based oxidation makes Co^{II}-PDI complexes, featuring electron-donating (methyl, methoxy, dimethylamine, thiomethyl) or electron-withdrawing groups (iodo, bromo, chloro) at the *para*, *meta*, or *ortho* positions of the terminal phenyl rings, promising candidates for use as molecular spin quantum capacitors storing and delivering charge in spintronic circuits, as depicted in Figure 5 [107]. Additionally, their high reversibility allows for repeated charging and discharging cycles without compromising performance.

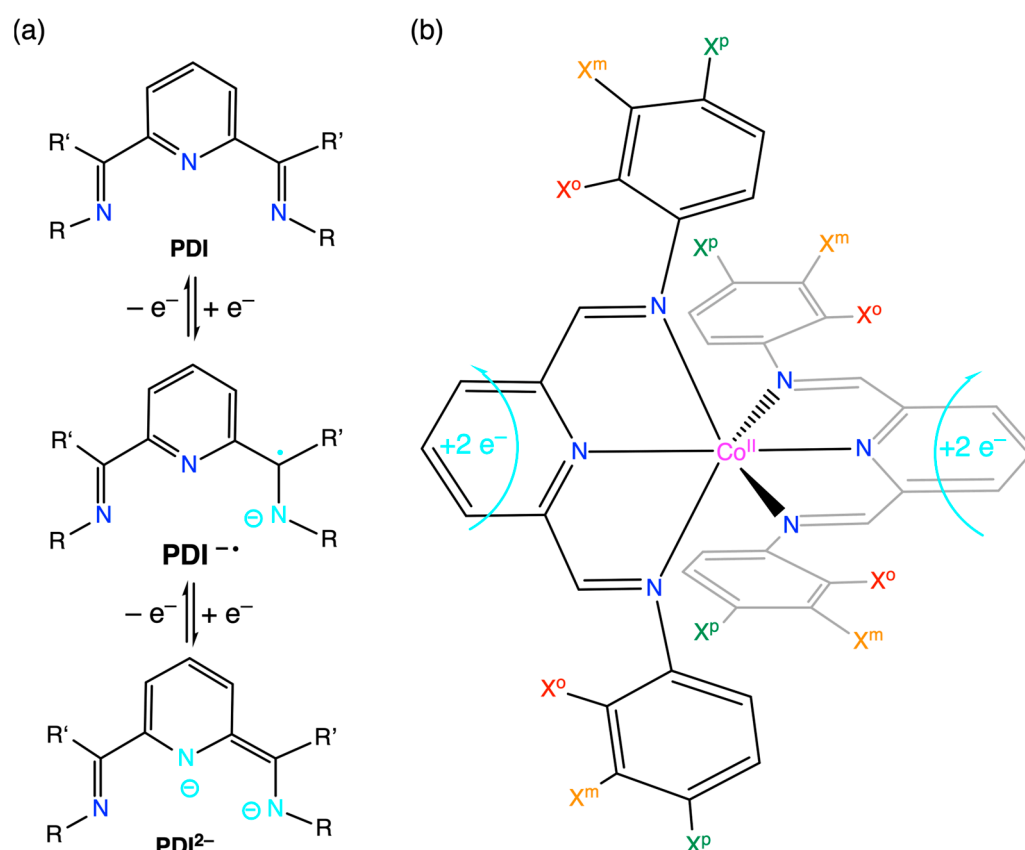


Figure 5. (a) Redox equilibria of PDI derivatives. (b) A schematic illustration of the potentiality of charge storage/delivery of the redox-active phenyl-substituted Co^{II}-PDI complexes proposed as a new class of molecular spin quantum capacitors.

Building on this concept, we will explore the idea of supercapacitors, which are relevant to molecules capable of storing energy and facilitating rapid, stable faradaic processes, such as charge and discharge cycles, to deliver substantial amounts of charge during circuit operations [116,117]. We propose the anthraquinone-substituted Co^{II} -PDI complex as a promising candidate, as illustrated in Figure 6. Anthraquinone (AQ) derivatives are well known for their π -acceptor character and redox chemistry, comprising quinone, semiquinone radical, and quinolate forms (Figure 6a) [118,119]. These anthraquinone moieties can serve as efficient multielectron reservoirs to develop a new class of charge storage spintronic devices: molecular spin quantum supercapacitors. Coupled with the PDI ligand, they could enhance the reduction capacity by two electrons per anthraquinone group, potentially allowing up to twelve ligand-based electron reductions within the Co^{II} -PDI complex (Figure 6b).

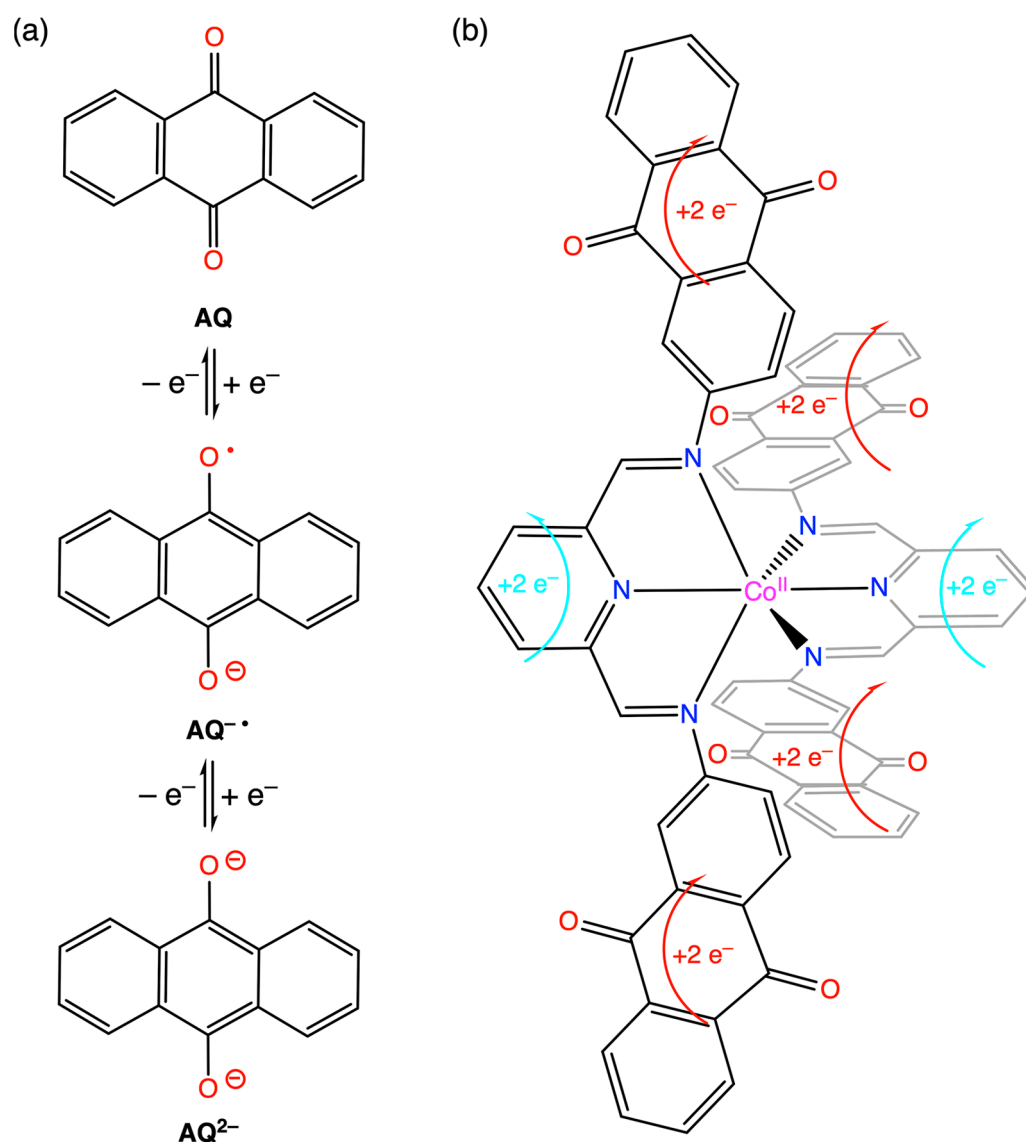


Figure 6. (a) Redox equilibria of anthraquinone in aprotic media. (b) A schematic illustration of the potentiality of charge storage/delivery of the redox-active anthraquinone-substituted Co^{II} -PDI complex proposed as a new class of molecular spin quantum supercapacitors.

2.1.2. Molecular Spin Quantum Chemo-, Electro-, or Photo-Switches

Molecular switches are essential components in any highly integrated molecular spintronic circuit, responsible for allowing and interrupting electron transport through the molecule by altering the molecular electronic state. Aware of this need, we propose the development of molecular switches whose spin state (LS or HS) and spin dynamics [fast (FR) or slow relaxation (SR)] can be triggered by means of chemical, electrochemical, and photonic stimuli, referred to as molecular spin quantum chemo- or electro- and photo-switches.

The ON–OFF electro-switching behavior of the *para*-methoxyphenyl-substituted Co^{II}-PDI complex, detailed in Figure 7, demonstrates how this Co^{II} SCO-SIM can work as a room-temperature molecular spin quantum electro-switch [104]. This complex can reversibly switch between the slow-relaxing paramagnetic LS Co^{II} ion (ON) and the diamagnetic LS Co^{III} ion (OFF) through chemical or electrochemical redox processes.

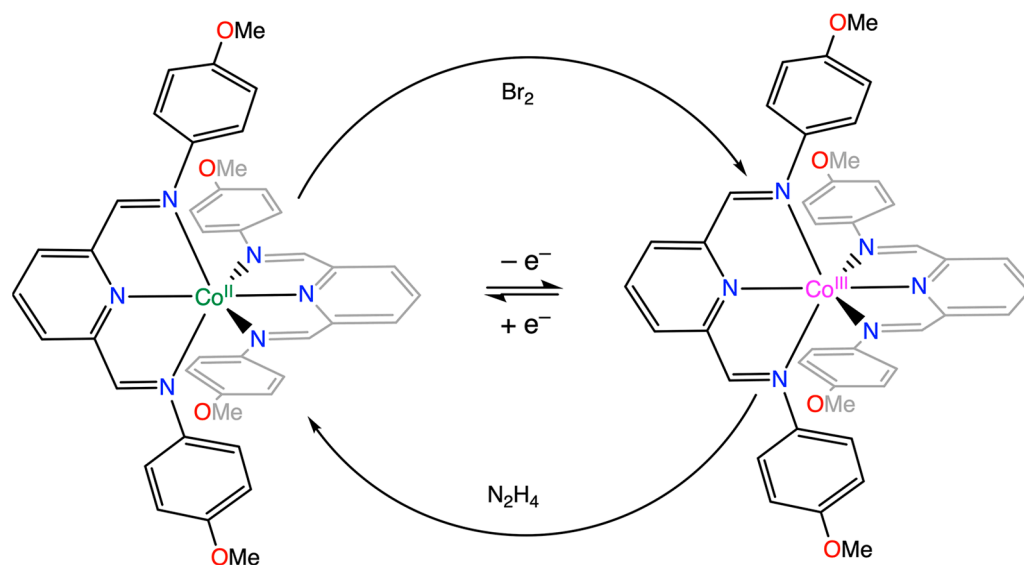


Figure 7. Reversible redox switching of *p*-methoxyphenyl-substituted Co^{II/III}-PDI complexes under chemical or electrochemical oxidation and reduction, as a new class of molecular spin quantum electro-switch.

The chemo-switching observed in the benzoic/benzoate-substituted Co^{II}-TERPY complexes inspired the second molecular spin quantum switch design, as illustrated in Figure 8 [105]. On them, we demonstrated how a single input, specifically a proton, can switch the redox, luminescent, and spin dynamic properties of a single molecule, while minimally affecting the SCO properties. A progressive enhancement of the luminescence in the ultraviolet (UV) region occurs upon deprotonation, concomitantly with a color change from orange to red, and is accompanied by a partial reversibility lost for the one-electron oxidation of the paramagnetic LS Co^{II} ion to the diamagnetic LS Co^{III} ion upon protonation. The dynamic equilibrium between the FS-protonated and SR-deprotonated forms of the LS Co^{II} ion illustrates well the whole potential of this advanced new class of pH-responsive electric, optical, and magnetic switches in the pursuit of multifunctional molecules that can serve as multiresponsive switches in highly integrated spintronic circuits.

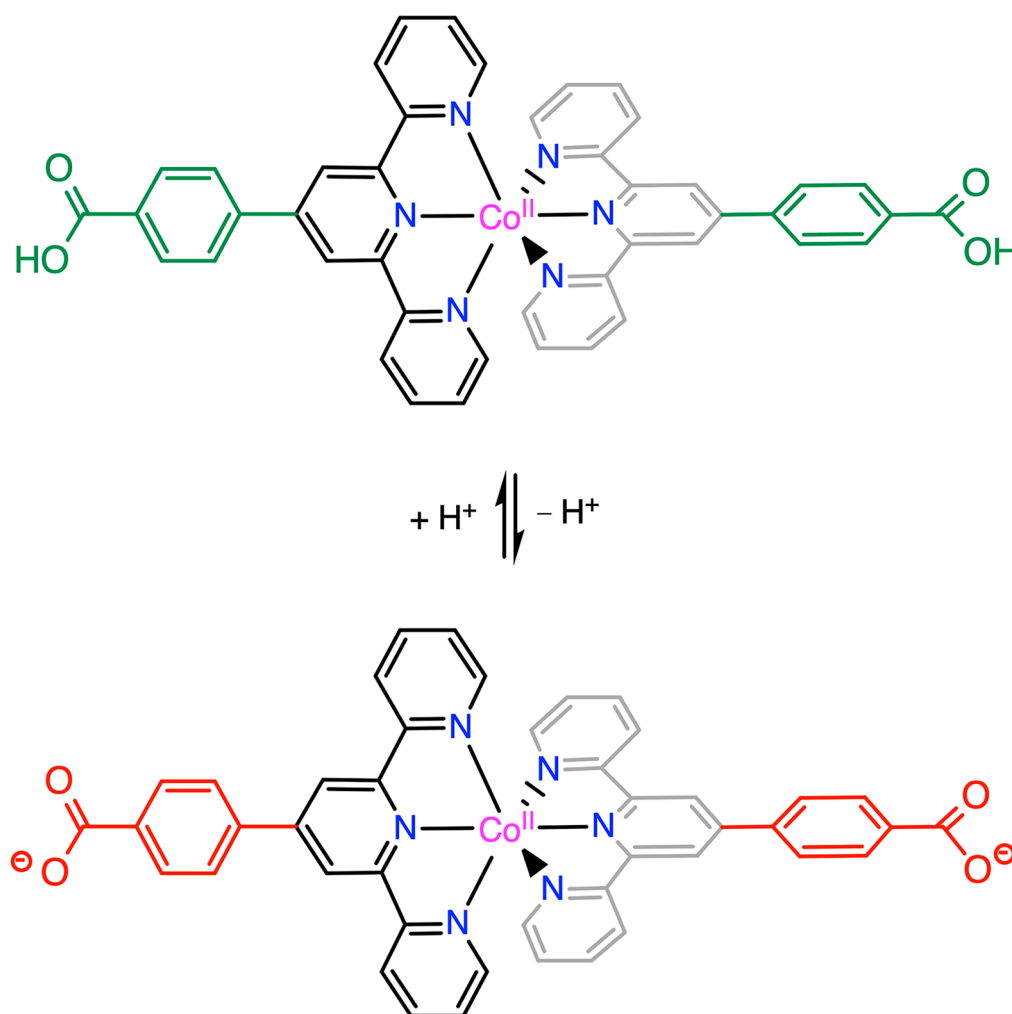


Figure 8. Reversible chemical switching of *p*-benzoic/benzoate-substituted Co^{II}-TERPY complexes under deprotonation and protonation, as a new class of molecular spin quantum chemo-switch.

The photo-control of magnetic properties along this family of cobalt(II)-TERPY complexes constitutes a major challenge for SMS, where SCO and photochemical properties converge, as well as SIM ones. Incorporating photoactive styryl or azophenyl substituents in the Co^{II}-TERPY complex, we can explore an innovative design of molecular switches focused on the well-known *cis-trans* (*Z-E*) photoisomerization reaction of styrene and azobenzene derivatives, as well as the duality of the magnetic relaxation dynamics of the Co^{II} ion depending on its electronic configuration, as illustrated in Figure 9. The LS OFF state ($S = 1/2$) and the HS ON state ($S = 3/2$) are a consequence of the changes in the ligand field strength caused by the variation in the aromaticity between planar *E* and non-planar *Z* configurations [120]. Our current efforts focus on further exploring this alternative ligand-driven, light-induced spin change (LD-LISC) route on these related pairs of photoactive stilbene- or azobenzene-substituted Co^{II}-TERPY complexes, provided that a significant variation between the LS and HS population can be observed upon UV and visible light irradiation.

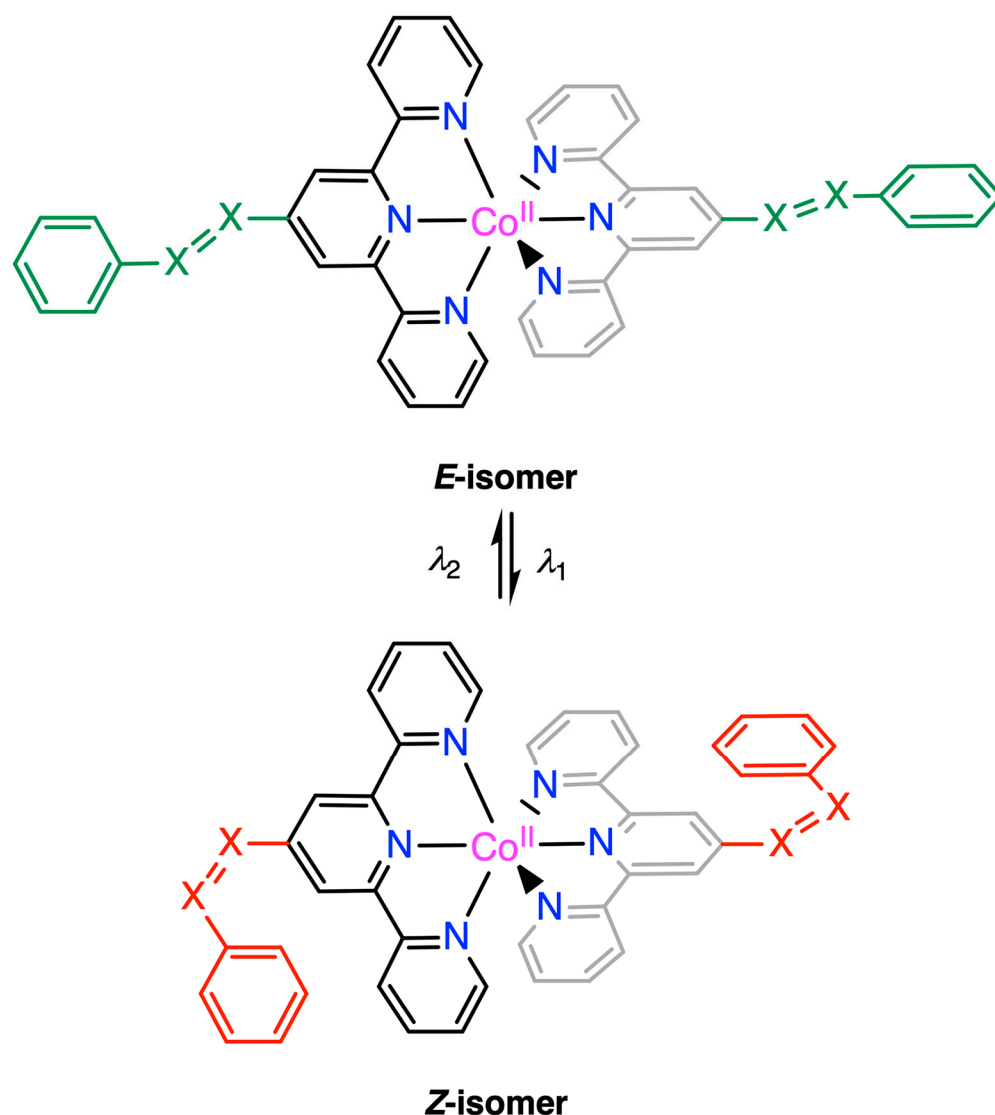


Figure 9. Photoisomerisation *cis-trans* (Z-E) equilibria of *p*-styryl- (X = CH) and *p*-azobenzene-substituted (X = N) Co^{II}-PDI complexes under UV and visible light irradiation, as a new class of molecular spin quantum photo-switches.

2.1.3. Chemo- and Electro-Switchable Molecular Spin Quantum Machines

We observed notable similarities between our Co^{II}-PDI complexes and the precursors of classical [2]catenane molecular machines, as illustrated in Figure 10. Both structures feature a mutually perpendicular arrangement of the coordinating-group PDI fragments, including reactive sites that enable the double-cyclization reaction.

The least risky strategy for synthesizing Co^{II}-PDI [2]catenanes begins with a pre-synthesized PDI macrocycle prior to the template reaction (Figure 10a). Then, by mixing the PDI macrocycle, Co^{II} ion, and open-chain PDI ligand in a 1:1:1 ratio, the only complex that forms is the desired intermediate (Figure 10b). In the final step, the open-chain fragment converts into another PDI macrocycle, resulting in two interlocked PDI rings [121,122]. At this stage, different approaches can be pursued depending on the functionality chosen for the potentially switchable molecular spin quantum machine. The versatility of these new systems is vast; for instance, the synthesis of a metal-based electro-switch using mixed TERPY/PDI macrocycles would integrate both platforms of cobalt(II) SCO-SIM complexes explored above (Figure 10c). Hopefully, the interplay could be triggered by

either a chemical or electrochemical oxidation on the metal ion, causing a sliding motion that enhances the stabilization of the Co^{III} ion in the TERPY coordination environment.

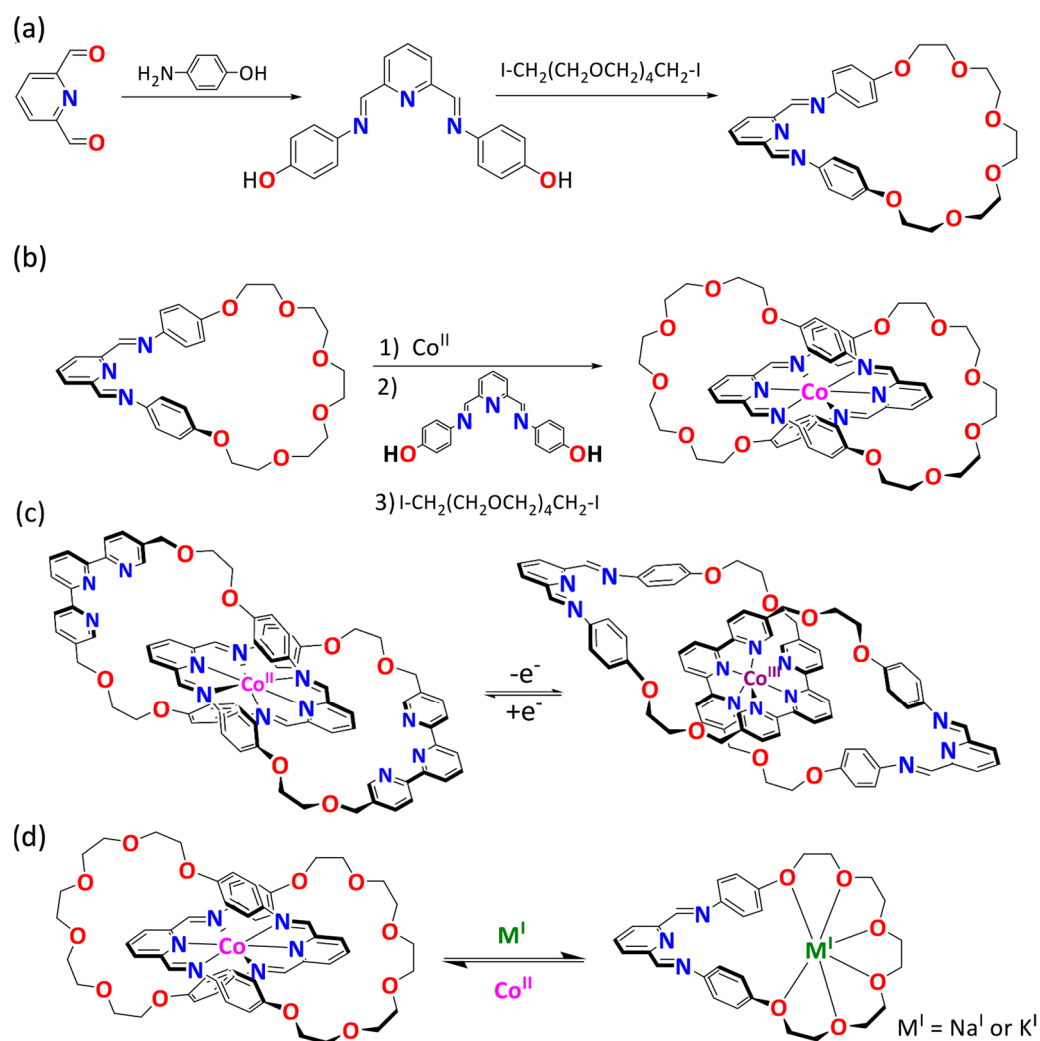


Figure 10. Proposed synthetic routes for (a) functionalized PDI macrocyclic and (b) catenane-type Co^{II} -PDI SCO-SIM complexes through a metal-directed template and double-cyclization reactions, leading to chemo- and photo-switchable molecular spin quantum machines. (c) The electrochemically or (d) chemically triggered sliding motion on mixed TERPY/PDI or pure PDI, catenane-type Co^{II} SCO-SIMs.

Ligand-based chemo-switches using these polyether-functionalized PDI macrocycles could interact with Na^+ and K^+ alkali cations, causing a sliding motion of the catenane and the subsequent release of the coordinated Co^{II} ion (Figure 10d). This feature evokes catenanes to work as molecular playgrounds for Na^+/K^+ and Co^{II} ions. When the Co^{II} ion is present, both SCO and SIM phenomena would be in the ON state, while high concentrations of alkali metal ions lead to the OFF state.

This innovative design may open up the path to a new class of mechanically bonded, catenane-type Co^{II} SCO-SIMs as unique examples of dynamic molecular systems with multiple switchable properties triggered by internal molecular motion.

2.2. Addressing of Co^{II} SCO-SIMs as Spin Quantum Nanodevices in SMS

The high expectations for this novel class of Co^{II} SCO-SIMs in data storage and processing stem from the potential to create spintronic devices in which these molecules

are uniformly organized across different inorganic and organic supports (e.g., silver, silicon, or graphene) while preserving their singular magnetic behavior [123–128].

The current challenge in the SMS area is addressing individual magnetic molecules into functional devices to study their spin-dependent electron transport properties. Basically, there are three approaches to address molecules for electron transport:

- (i) Electrode-based junctions: Placing molecules between two electrodes and measuring the conductance across the device.
- (ii) Scanning tunneling microscopy (STM): Depositing molecules on a surface and using an STM tip as a lead to measure the electron transport properties across the individual molecule.
- (iii) Nanostructure integration: Anchoring molecules to carbon-based nanostructures through supramolecular interactions, using molecules for their spin, while electron transport occurs through the quantum dot or the carbon nanostructure.

Recent research has yielded promising prototypes of spintronic devices based on either SCO or SIM molecules from these three strategies (see the Introduction and Background Section).

Due to their nanometer size and ease of handling, the Co^{II} SCO-SIM compounds that constitute the leitmotif of this perspective review appear as suitable candidates for the study of spin dependence of the electron transport through single molecules, envisaging the magnetic control of conduction properties or vice versa, the electric control of magnetic properties. Let us briefly anticipate some of the expected results as spin quantum transistors, filters, or valves for single-molecule electron transport, which can be achieved with this variety of SCO molecular nanomagnets when they are connected to two gold electrodes, attached to a gold surface, integrated in a SWCNT, or anchored on a nanographene (NG).

2.2.1. Molecular Spin Quantum Transistors in Gold Molecular Junctions

The observed capacitor-like redox behavior in the class of cobalt(II)-PDI SCO-SIMs allows us to propose them as prototypes of electric field-effect spin quantum transistors (EFE-SQTs) in SMS [64]. So, for instance, the 4-thiomethylphenyl-substituted Co^{II}-4-MeSPhPDI complex is a very appealing candidate due to its strong affinity for gold electrodes via the sulfur atoms of the thiomethyl substituents, as illustrated in Figure 11 [107]. Two opposite thiomethyl substituents from one ligand would connect to the source and drain electrodes, establishing the electron flux (Figure 11a). Depending on the applied electric voltage, dramatic changes in the electrical conductances can be then presumed when passing from the HS ($S = 3/2$) or LS ($S = 1/2$) cobalt(II) complex, [Co^{II}(4-MeSPhPDI)₂]²⁺ to the antiferro- ($S = 1/2$) or ferromagnetically coupled ($S = 3/2$) metal-diradical reduced species, [Co^{II}(4-MeSPhPDI^{•-})₂], as previously reported for the related Fe^{II}-DPZBPY SCO complex [63].

As with most transition metal-based SIMs, the presence of a fast quantum tunneling of magnetization (QTM) in our cobalt(II) SCO-SIMs under a zero applied *dc* magnetic field offers an alternative and highly efficient relaxation mechanism that severely limits their use in high-density information storage devices. Otherwise, the considerable decrease in the magnetic relaxation rate with an increasing external magnetic field observed in most LS cobalt(II) SIMs could be exploited to develop a new class of magnetic field-effect spin quantum transistors (MFE-SQTs) for applications in SMS [106]. In contrast to conventional electronic devices controlled by an electric field, the electrical current flow, in such cases, would be governed by a magnetic field. Indeed, different electrical conductances can be expected for FR and SR LS Co^{II} ions, occurring in the absence or presence of an external magnetic field. Although this approach to operating on a device involves a greater degree of difficulty than using an electric current due to the challenge of confining a magnetic field to a nanometric or smaller region, Bogani and Ruben demonstrated that this was possible by creating supramolecular SVQs [73].

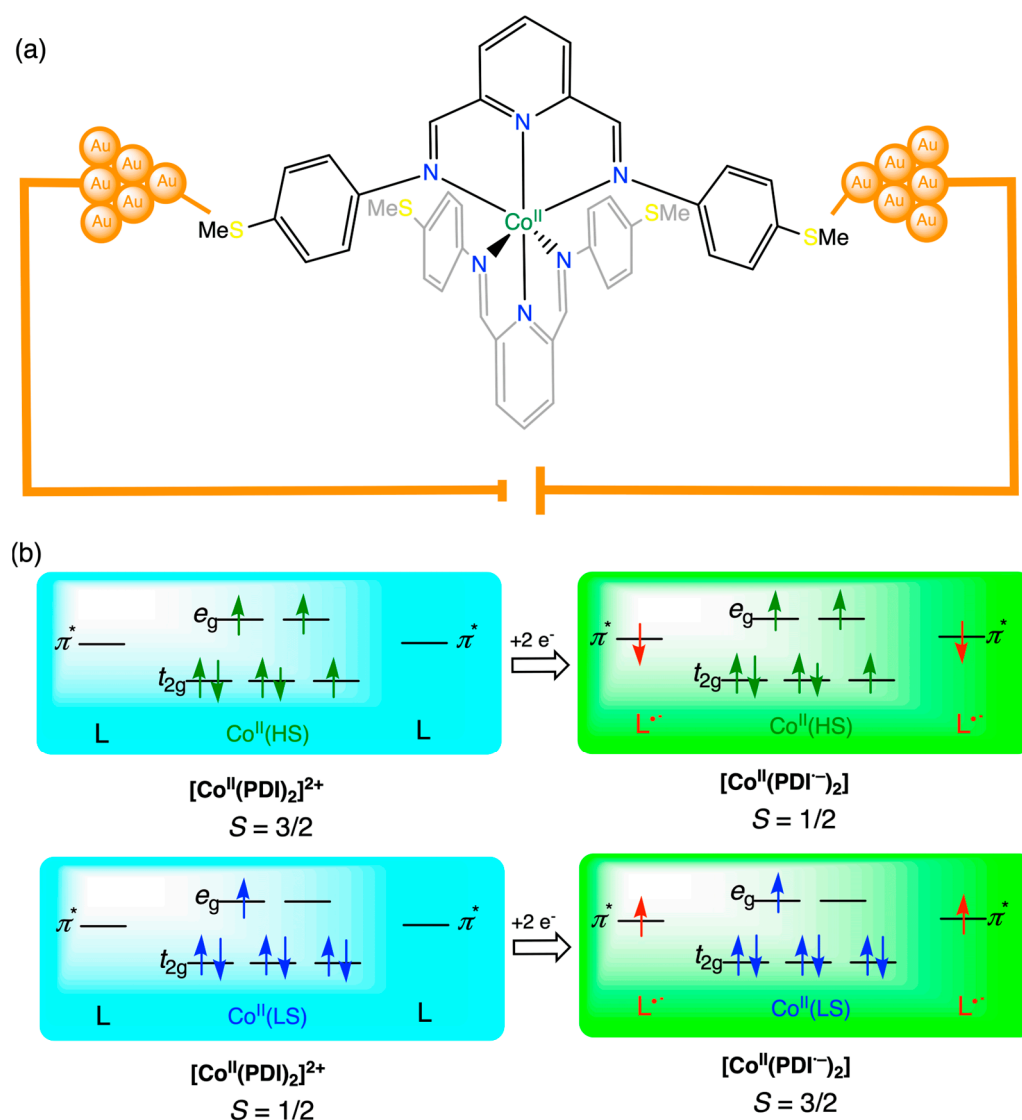


Figure 11. (a) An illustration of the proposed molecular junction device constructed by the 4-thiomethylphenyl-substituted Co^{II} -PDI complex connecting two gold electrodes as a prototype of the electric field-effect spin quantum transistor. (b) A simplified energy level diagram of the interaction between the d-type metal orbitals and the π^* -type ligand orbitals for the HS (top) and LS (bottom) Co^{II} forms of the cationic $[Co^{II}(PDI)_2]^{2+}$ complex and the corresponding doubly reduced neutral $[Co^{II}(PDI^{\bullet-})_2]$ species, illustrating the charge-induced electro-switching magnetic behavior.

2.2.2. Molecular Spin Quantum Filters in Gold Surfaces

Within this context, the electroactive Co^{II} -PDI complexes with electron-donor thiomethyl substituents on the terminal phenyl rings offer a promising platform for developing a new class of spin quantum filters (SQFs), which is due to several factors:

- (i) The sulfur atoms have a large affinity for various metallic substrates.
- (ii) The spin dynamic properties can be tuned when an external magnetic field is applied, similar to the behavior of bulk materials.
- (iii) The electrochemical activity associated with metal oxidation can work as an ON-OFF switch for the spin filter device.

Consequently, while the paramagnetic HS Co^{II} ion in the ON state would filter spin-up (α) electrons, the diamagnetic LS Co^{III} ion in the OFF state would lack any selectivity in distinguishing spin-polarized electrons, as previously reported for the isoelectronic diamagnetic LS Fe^{II} -BEPYDMP complex (see Figure 2) [67].

The chiral-induced spin-selectivity (CISS) effect links chiral symmetry directly to the electron spin within molecules, evident through phenomena such as electron transmission and displacement currents driven by charge polarization that subsequently induce spin polarization [129]. Consequently, the traditional definition of the OFF state needs to change when considering chiral molecules; what was previously deemed OFF now forms the foundation for chiral spin filters, thereby expanding the scope of spintronic applications. However, the previous OFF state is expected to show an attenuated spin polarization concerning the ON state [130], which can be used to design memristors that are resistance-switching memory devices capable of mimicking biological synaptic functions in artificial neural networks [131].

2.2.3. Molecular Spin Quantum Valves in Carbon-Based Nanostructures

Hybrid carbon-based materials play a crucial role in enhancing and thoroughly exploring the spin dynamic properties of SIMs. Recognizing this potential, Bogani and Ruben proposed anchoring a lanthanide-based SIM onto an SWCNT [70,71]. Achieving this required a rational-designed SIM incorporating anchoring groups capable of engaging in supramolecular π - π interactions with the SWCNT (see Figure 4). In their pioneering work, Bogani and Ruben successfully self-assembled a heteroleptic derivative of the archetypical double-decker [Tb(PC)₂], bearing one modified pyrene and six hexyl groups, onto the SWCNT (see Figure 4) [72]. From these results, a new molecular spintronic device emerged: the supramolecular spin quantum valve (SQV) [73].

Mononuclear Co^{II}-PDI complexes with oligoacene (naphthalene and anthracene) substituents would be suitable for preparing these hybrid metalcarbon nanotube and nanographene architectures. However, a more advantageous option might be Co^{II}-PDI derivatives incorporating extended aromatic anchoring groups, like pyrene or its derivatives, along with flexible aliphatic linkers, as depicted in Figure 12.

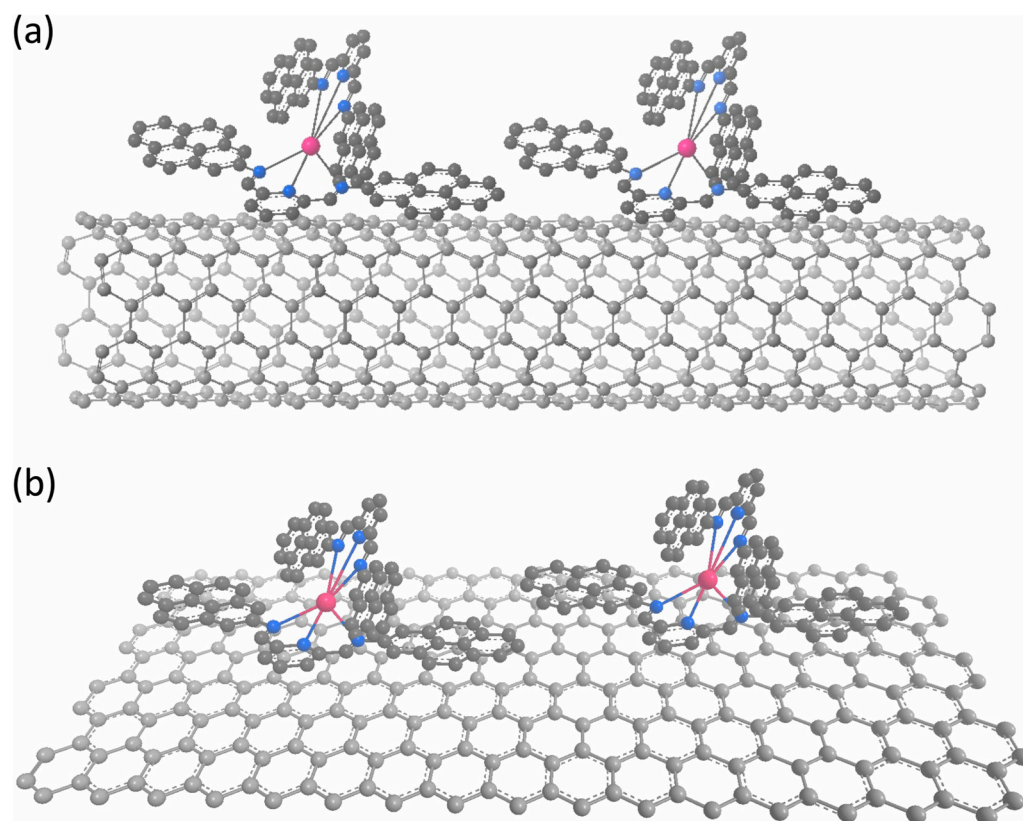


Figure 12. Illustration of the supramolecular carbon-based nanotubes (a) and nanographenes (b) with pyrene-substituted Co^{II}-PDI complexes as prototypes of molecular spin quantum valves.

2.3. Scaling of Co^{II} SCO-SIMs as Spin Quantum Nanodevices in QIP

A molecular approach to quantum computing nanotechnologies can be likened to a three-tiered process, analogous to the bottom-up strategy employed in supramolecular chemistry. Each step progressively increases complexity, culminating in constructing the desired material. These stages can be summarized as follows:

- (i) Designing qubits with exceptional quantum coherence;
- (ii) Scaling up to implement double qubit-based quantum gates (QGs);
- (iii) Conceiving a quantum computing device as a multiqubit 2D array capable of storing and processing quantum information.

While significant strides have been made in designing and controlling qubits, both individually and within QGs, the final stage, representing the ultimate objective, remains largely unexplored.

In the quest to minimize quantum decoherence, several promising candidates for molecular-based qubits have emerged, incorporating many first-row transition metal ions from vanadium to copper [132–139]. These include the octahedral vanadium(IV), iron(III), and chromium(III) complexes of formula $[V(C_8S_8)_3]^{2-}$, $[Fe(C_5O_5)_3]^{3-}$, and $[Cr(C_3S_5)_2]^{3-}$, in which only nuclear spin-free elements (C, O, and S) compose the ligands [132–134]. This feature, combined with the low abundance of nuclear spin-active isotopes in these elements, grants long coherence times (T_2 or T_m) once nuclear spins are the main source of magnetic noise and thus decoherence. Changing the chemical matrix to a spin-free solvent like CS₂ or SO₂ made it possible to increase T_2 up to 675 μ s at 10 K for $[V(C_8S_8)_3]^{2-}$ [132]. In contrast, the related square-pyramidal oxovanadium(IV) complex, $[VO(C_8S_8)_2]^{2-}$, exhibited a slight decrease in T_2 to 104 μ s at 10 K in SO₂ [135]. Other remarkable candidates for the qubit include the square-pyramidal oxovanadium(IV)-phthalocyanine [VO(PC)] and square-planar copper(II)-maleonitriledithiolate $[Cu(MNT)_2]^{2-}$ complexes, owing T_2 values of 1 μ s at room temperature, despite placing donor or nuclear spin-active isotope (N) atoms close to the metal center [136,137].

Scalability is essential in the development of spin-based quantum computing. This term, closely related to entanglement, refers to the ability to increase the number of qubits in arrays while preserving the capacity to manipulate and read out information without compromising quantum coherence. This topic is a challenging step in the development of a spin-based quantum computer. Each array has its own advantages and disadvantages, making it essential to have a versatile and easy-to-handle qubit platform that may be processed in various architectures, such as our Co^{II}-TERPY and Co^{II}-PDI complexes, illustrated in Figure 13. To follow, we provide some attempts to exemplify the potential and versatility in designing, scaling, and addressing cobalt(II) SCO-SIMs discussed in this review as building components for quantum computing technologies. In this context, new constructions could be achieved through diverse supramolecular cobalt(II) SCO-SIM architectures obtained through ligand design.

Our results may open a pathway toward the design of operative molecular spin qubits or qubit arrays projecting the physical implementation of a new class of multifunctional electrical, optical, chemical, and magnetic materials for QIP. After identifying the key design criteria to improve the SCO and SIM performance of our mononuclear cobalt(II) complexes, two critical challenges should be addressed to achieve this goal:

- (i) Pinpointing the primary sources of quantum decoherence in cobalt(II) SCO-SIMs;
- (ii) Building supramolecular arrays of cobalt(II) SCO-SIMs with increasing complexity, featuring non-negligible feeble and potentially switchable intermolecular interactions;
- (iii) Effectively addressing suitable cobalt(II) SCO-SIMs and their supramolecular arrays on surfaces and other solid supports.

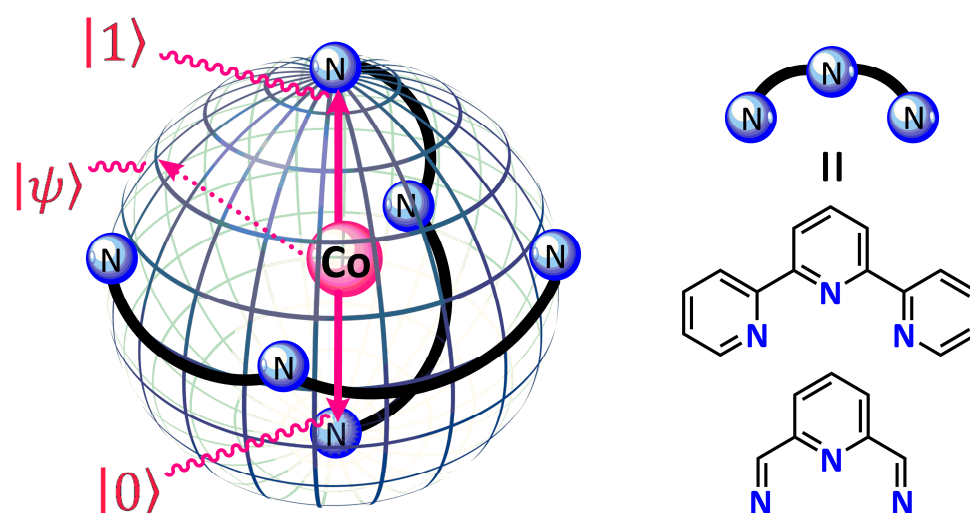


Figure 13. Selected TERPY and PDI platforms for the creation of a new chemical library of Co^{II} SCO-SIM molecules as candidates to molecular spin quantum bits.

2.3.1. Molecular Spin Quantum Bits

In cobalt(II) SCO-SIMs, the LS Co^{II} ion is a genuine two-level magnetic quantum system represented by the $m_S = +1/2$ and $-1/2$ states, which can play the role of the superposed 0 and 1 states in a qubit for quantum computing applications. In contrast, due to significant first-order spin-orbit coupling (SOC), the HS state possesses an effective doublet ground spin state ($S_{\text{eff}} = 1/2$) coming from the ground $m_S = \pm 1/2$ or $m_S = \pm 3/2$ Kramers doublet for an easy-plane ($D > 0$) or easy-axis ($D < 0$) magnetic anisotropy, respectively. As a matter of fact, the slow magnetic relaxation behavior, along with this family of SCO cobalt(II)-TERPY and PDI complexes, is dominated by single or double Raman mechanisms between the $m_S = +1/2$ and $-1/2$ states [LS or HS ($D > 0$)] or $m_S = +3/2$ and $-3/2$ states [HS ($D < 0$)] through a virtual excited state, with no participation of Orbach one through the excited $m_S = +1/2$ and $-1/2$ states in the latter case, and occasionally with additional temperature-independent Intra-Kramer [LS or HS ($D > 0$)] or QTM mechanisms [HS ($D < 0$)] [105–107].

Typically, the magnetic relaxation time for a doublet spin ground state is equivalent to the spin-lattice time ($T_1 = \tau$), which acts as a limiting factor for the phase memory time ($T_m \leq T_1$). Our octahedral LS Co^{II} -TERPY and Co^{II} -PDI complexes exhibit promising T_1 values at 2.0 K, ranging from 100 μs to 1 ms [105–107]. However, these values are slightly lower than those reported for some square-planar LS cobalt(II) complexes (1.3 and 11.1 ms at 2.0 K), specifically $[\text{Co}(\text{TMC})(\text{CH}_3\text{CN})]^{2+}$ and $[\text{Co}(\text{PC})]$, where TMC = 1,4,7,10-tetramethyl-1,4,7,10-tetraazacyclododecane [101,138]. However, complete pulsed EPR studies should be performed on both LS and HS complexes to characterize and assess their suitability as new candidates for spin qubits.

Recently, our research group has focused on pulsed EPR studies of octahedral HS cobalt(II) complex $[\text{Co}(\text{DMPHEN})_2(\text{SAL})]^+$ (DMPHEN = 2,9-dimethyl-1-10-phenanthroline; SAL = salicylaldehyde) with a positive D value ($S = 3/2$) [139]. In this case, due to the strong SOC contribution, the T_1 rapidly decreases as the temperature increases. Yet, the T_m value for this complex is somehow comparable to other qubit candidates (around 1 μs at 2.0 K) [132–137], which is a good relaxation time for this low temperature. Notably, the dc and ac magnetic or cw-EPR characteristics of this complex are similar to those of our HS cobalt(II)-PDI complexes with *p*-chlorophenyl and *p*-thiomethylphenyl substituents (see Figure 5), positioning them as potential candidates for molecular spin quantum bits.

2.3.2. Optically, Chemically or Electrochemically, and Electrically or Magnetically Addressable Molecular Spin Quantum Bits

These distinctive multifunctional and multiresponsive Co^{II} SCO-SIMs appear as up-and-coming candidates for the multiple (optical, chemical or electrochemical, and electrical or magnetic) qubits addressing in future QIP applications. The results herein presented constitute an important step in the pursuit of advanced addressable qubits and the controlled resetting of the quantum gate.

All the compounds discussed here are attractive for developing advanced qubits with electrical readout capabilities. The electro-switching from the paramagnetic LS/HS Co^{II} state to the diamagnetic Co^{III} state of the active metal center offers an excellent opportunity to erase and reinitiate the qubit at the conclusion and beginning of information processing. Furthermore, when exposed to a suitable combination of two or more stimuli—such as an external magnetic field, electrical voltage at the gate, light irradiation, and pH— Co^{II} SCO-SIM compounds can act as quantum logic gates processing all the inputs into a single output.

In the search for ideal qubits, there is a consensus that the all optically addressable qubits are particularly advantageous for several reasons:

- (i) Light is an environmentally green stimulus;
- (ii) They can be remotely controlled with precision timing and positioning;
- (iii) They enable straightforward single-spin readout and initialization;
- (iv) They can be orthogonally coupled with other switchable entities in a single-spin configuration to build complex logic multitaskers.

This appealing need within the field of quantum computing field moved us to invest efforts in creating and studying a family of optically active Co^{II} SCO-SIMs by simply incorporating oligoacene luminophore groups, such as naphthalene or anthracene, into our Co^{II} -PDI platform, as illustrated in Figure 14. A preliminary study of their photophysical activity in solution reveals significant metal-promoted quenching of the ligand luminescence upon UV light irradiation at room temperature, likely due to a ligand-to-metal charge transfer (LMCT) process that leads to a short-lived excited state of the Co^{II} ion, analogous to the LIESST excited state, which is not readily accessible in our Co^{II} SCO-SIM [140].

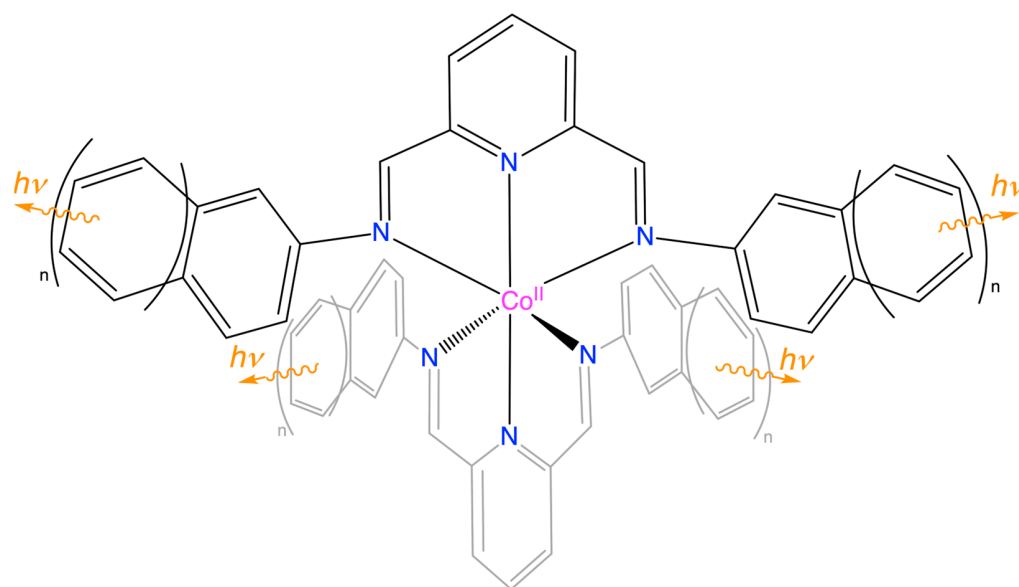


Figure 14. A schematic illustration of the potentiality of luminescent 2-naphthalene- ($n = 2$) and 2-anthracene-substituted ($n = 3$) Co^{II} -PDI complexes proposed as a new class of optically addressable molecular spin quantum bits.

In this regard, the parent Co^{II} -TERPY complex exhibits ultrafast Jahn-Teller (JT) photo-switching behavior in aqueous solution, transitioning between axially elongated LS and axially compressed HS forms on the femtosecond timescale upon optical metal-to-ligand charge transfer (MLCT) excitation at room temperature under deep violet-blue light [108]. The photo-control of magnetic properties along this family of cobalt(II)-TERPY complexes constitutes a major challenge for SMS, where SCO and photophysical properties converge, as do SIM ones. Moreover, this finding opens new exciting perspectives for implementing logic schemes in QIP through the optical control of quantum coherence (QC) properties of multiresponsive Co^{II} SCO-SIMs as prototypes of optically addressable qubits, provided that the lifetimes of the photogenerated metastable states are sufficiently long relative to the typical manipulation time of about 10 ns for a qubit.

2.3.3. Exotic Arrays of Molecular Spin Quantum Bits in Soft Matter

Once most sources of quantum decoherence in solution or a solid state (diluted solid solutions) are identified, further investigations into Co^{II} SCO-SIMs in soft media will benefit their potential applications in QIP.

Although some questions about the SCO and SIM behaviors in crystalline solids remain unclear, these topics are still largely studied. This is different when it comes to soft matter. Bulk assemblies such as colloids, liquid crystals, polymers, vesicles, and Langmuir–Blodgett (LB) films incorporating SCO and SIM behaviors remain largely uncharted territory. However, the few works reported in this area provided promising results regarding improving SCO behavior. Examples of this feature include the LB films based on an amphiphilic iron(II) complex, $[\text{Fe}([\text{CH}_3(\text{CH}_2)_{16}]_2\text{BBY})_2(\text{NCS})_2]$ ($[\text{CH}_3(\text{CH}_2)_{16}]_2\text{BBY} = 4,4'$ -diheptadecyl-2,2'-bipyridine), which exhibits thermally assisted cycle-dependent SCO [141,142]. This atypical behavior is attributed to the melting of the alkyl chain groups, aiding in reorganizing the structure to favor the SCO process. Additionally, Sun et al. prepared SCO vesicular nanospheres based on the series of neutral iron(II) complexes with 2,2'-bipyridine-4,4'-dicarboxamide ligands bearing different alkyl group substituents, ranging from propyl to cetyl (R_2BPYCA with $\text{R} = \text{CH}_3(\text{CH}_2)_n$ and $n = 2-15$), represented by the general formula $[\text{Fe}(\text{BPZ})_2(\text{R}_2\text{BPYCA})]$ [$\text{BPZ} = \text{dihydrobis}(1\text{-pyrazolyl})\text{borate}$] [143]. The spin transition temperature of the vesicular nanospheres was significantly shifted from 160 K for the bulk material to room temperature [143].

Another intriguing example is the cobalt(II) complex $[\text{Co}(\text{C}_{16}\text{-TERPY})_2]^{2+}$, which evinces an unexpected reverse spin transition triggered by a structural vitreous phase transition [144]; however, the possible SIM behavior based on the reverse HS state was unfortunately not studied. In this context, mononuclear Co^{II} -PDI and TERPY complexes with long polyalkyl substituents offer a suitable Co^{II} SCO-SIM platform for studying both phenomena and, ultimately, for testing their qubit performance in soft matter for the first time, as depicted in Figure 15.

2.3.4. Molecular Spin Quantum Bits in Porous MOF-Based Materials

An original approach to address individual spin-crossover cobalt(II) molecular nanomagnets within matrixes would be to take advantage of the combined host–guest chemistry and geometrical features of metal–organic frameworks (MOFs) to produce a new class of hybrid materials. MOFs have been extensively studied for their applications in gas storage and separation, drug delivery, molecular recognition, transport and catalysis, as well as for their use as a template for the growth of nanoparticles and the encapsulation of a wide variety of functional moieties [145–149].

Owing to their porosity and rich host–guest chemistry, MOFs are excellent playgrounds for designing multifunctional and multiresponsive hybrid materials by hosting Co^{II} SCO-SIMs on pre-existent MOF matrices. This setup allows for the investigation of quantum decoherence in a confined environment of the adsorbed Co^{II} SCO-SIM, the results of which will be compared with those obtained in solution, a solid state, or soft matter to optimize their performance as qubits for future applications in QIP.

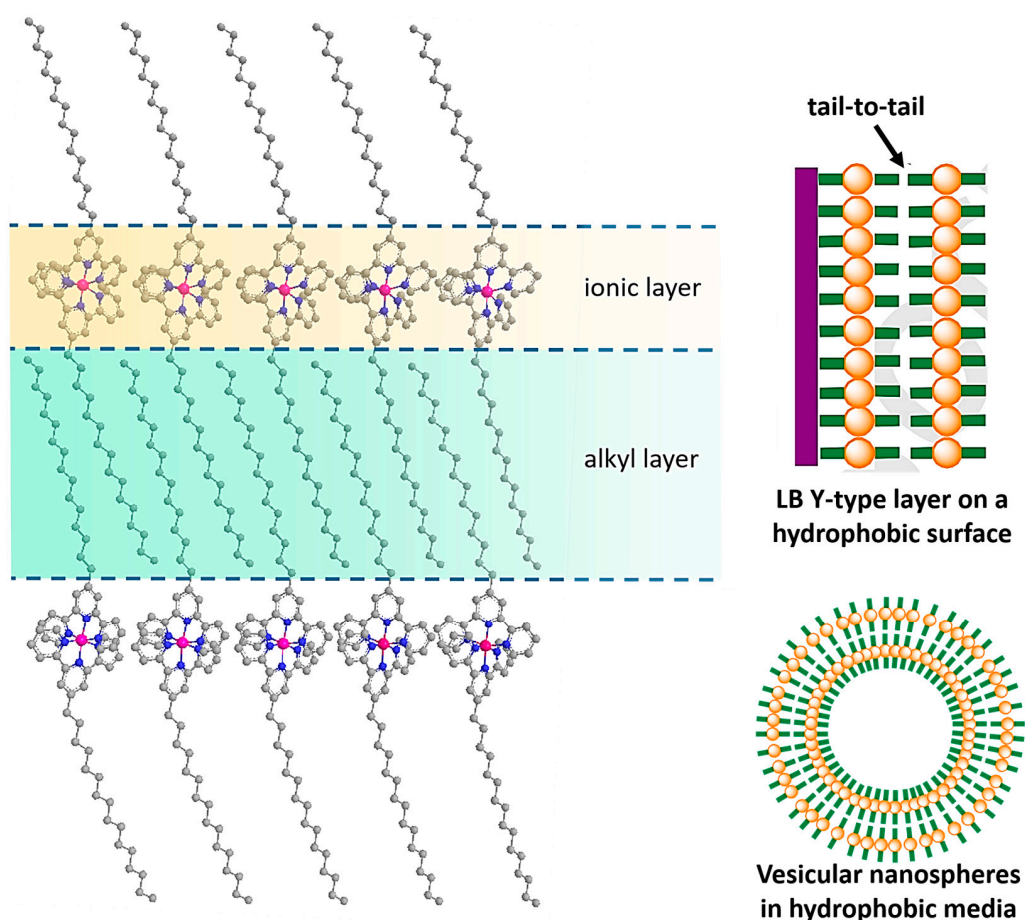


Figure 15. Examples of LB films and vesicular nanospheres from Co^{II} SCO-SIMs with long polyalkyl-substituted TERPY ligands as building blocks for exotic arrays of entangled and potentially switchable molecular spin quantum qubits.

Additionally, the long-range magnetic ordering from the magnetic MOF host can influence the slow magnetic relaxation of the incorporated Co^{II} SCO-SIM guests, resulting in a synergistic interplay of both magnetic phenomena. Previously, our research group reported the partial incorporation of cationic iron(III)-Schiff's base SCO and manganese(III)-porphyrin SIM complexes into the large channels of an anionic oxamato-based copper(II)-manganese(II) 3D MOF of formula $\text{Na}_4\{\text{Mn}_4[\text{Cu}_2(\text{TMMMPBA})_2]_3\} \cdot 60\text{H}_2\text{O}$ [TMMMPBA = *N,N'*-2,4,6-trimethyl-1,3-phenylenebis(oxamate)] via cation-exchange single-crystal-to-single-crystal (SC-SC) processes [150–152]. The resulting host–guest hybrid materials exhibited hysteretic SCO behavior or internal field-induced partial quenching of the QTM of the iron(III) and manganese(III) guests, respectively [151,152]. These features constitute unique proofs of the synergistic effects between the spin dynamics of the guests and the long-range magnetic ordering of the host, demonstrating that this class of porous magnets is a well-suited platform for the controlled addressing of SIMs.

There again, our preliminary studies revealed that the parent cationic Co^{II} SCO-SIM complex $[\text{Co}^{\text{II}}(\text{PhPDI})_2]^{2+}$ could be hosted within the large pores of the aforementioned anionic ferrimagnetic copper(II)-manganese(II) MOF, as illustrated in Figure 16 [140]. Energy-dispersive X-ray (EDX) analysis indicates that all exchangeable Na^{I} ions were successfully replaced by the new $[\text{Co}^{\text{II}}(\text{PhPDI})_2]^{2+}$ guest over the course of one week. This promising result offers a new perspective on how SCO and SIM behaviors could be modulated by addressing the spin carriers as hybrid materials. Moving forward, we plan to investigate quantum decoherence through pulsed EPR experiments on partially exchanged diluted samples of the $[\text{Co}^{\text{II}}(\text{PhPDI})_2]^{2+}$ complex adsorbed into a diamagnetic nickel(II)-magnesium(II) MOF derivative.

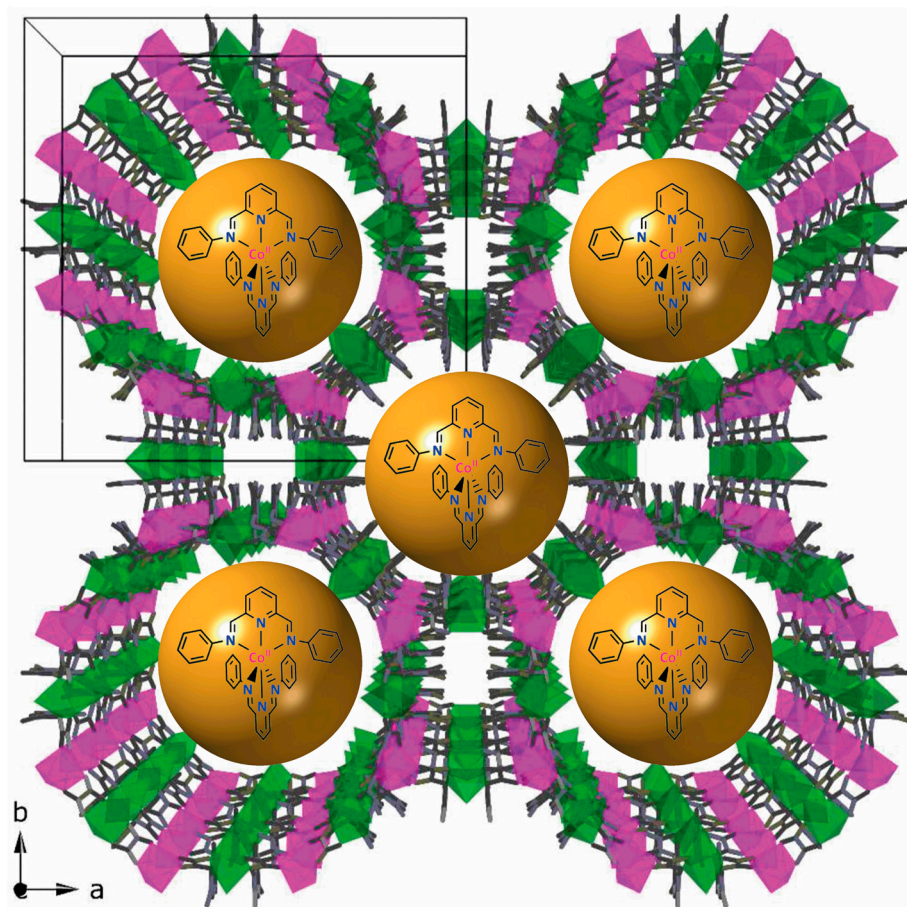


Figure 16. Illustrative representation of the chemisorption of the Co^{II} -PDI complexes into the giant pores of the anionic MOF of formula $\{\text{Mn}_4[\text{Cu}_2(\text{TMMMPBA})_2]_3\}^{4-}$ as building blocks for arrays of molecular spin quantum qubits.

2.3.5. MOFs and MCOFs as Entangled and Potentially Switchable Ordered Arrays of Molecular Spin Quantum Bits

Designing and synthesizing weakly interacting (entangled) and potentially switchable ordered arrays of qubits is mandatory for constructing a quantum computer, as depicted in Figure 17. Hence, the Sycamore processor, a commercial quantum computer realized under Feynman's vision, is based on microscopic superconducting circuits arranged in a square grid array of 54 qubits (53 operatives), each connected to its four nearest neighbors with appropriate couplers [6]. Inspired by this achievement, we believe that the challenges of spin-based quantum computing machines could be addressed shortly by applying the principles of reticular chemistry (Figure 17) [153].

MOFs made of metal ions or small metal clusters serving as secondary building units (SBUs) linked by a diverse range of organic spacers are particularly well suited for this purpose [154,155]. We have demonstrated that the bottom-up “complex as ligand” approach is an effective method for creating new mixed-metal MOFs and, in some instances, the resulting thin films of these MOFs [156,157]. In fact, metal complexes with additional coordinating groups function as ligands (metalloligands) toward other metal ions, forming high-dimensional 2D and 3D MOF structures.

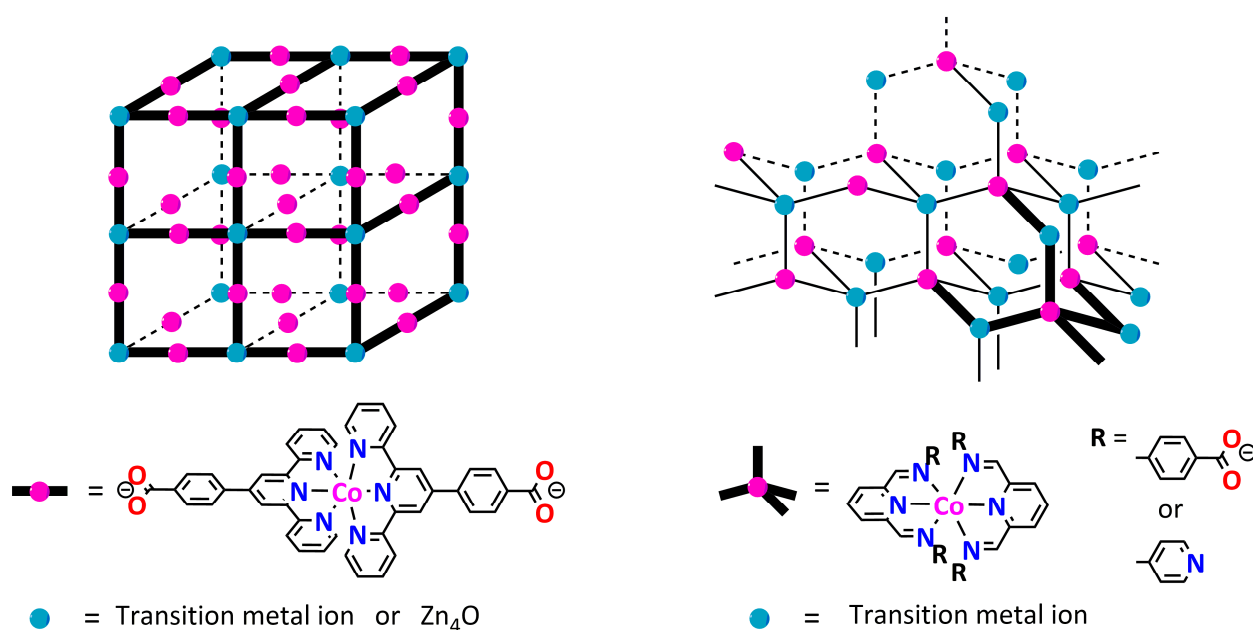


Figure 17. Illustration of the proposed 3D MOFs of cubic or diamond topologies built from mononuclear cobalt(II) SCO-SIM complexes with benzoate- or pyridine-substituted TERPY and PDI ligands as linkers towards transition metal ions or clusters as SBUs for arrays of entangled and potentially switchable molecular spin quantum qubits.

In this regard, the Co^{II} -TERPY and Co^{II} -PDI SCO-SIM complexes discussed in this review are promising metalloligands for constructing mixed-metal MOFs since, by modifying peripheral substituents, these complexes can be tailored to match the Lewis acidity of different metal ions, leading to nD (where $n = 2$ or 3) SCO-SIM networks. Oxygen-donor benzoate groups coordinate to hard ions like lanthanides, while nitrogen-donor groups from pyridines are appropriate for interacting with many first-row transition metals of interest. In addition, the different directional nature of these metalloligands favors the formation of different 3D MOF topologies, such as cubic (for Co^{II} -TERPY) or diamond-type (for Co^{II} -PDI), where the cobalt(II) complexes occupy the edges, and the second metal ion (or SBU) occupies the nodes (see Figure 17). It is worth noting that our benzoate-substituted TERPY cobalt(II) complex (see Figure 8), significantly longer than the conventional aromatic dicarboxylates used in Yaghi's MOFs [154,155], would enhance the porosity of the new material.

Covalent organic frameworks (COFs) resulting from the linking of organic building units through well-established organic reactions (e.g., C=N imine formation), and, eventually, their metal-containing derivatives, so-called metal-covalent organic frameworks (MCOFs), are now emerging as propitious alternatives to MOFs, representing unique examples of porous crystalline hybrid materials [158,159]. Among COFs, those with interlaced structures—created through the self-assembly of molecular organic building blocks into linear organic strands woven in two or three dimensions—mean a major challenge for organic chemists. A clever approach to achieving interlaced structures involves using metal ions with specific stereochemical preferences to template the polymerization reaction, resulting in an ordered woven pattern in the MCOF, provided that the organic building blocks include the required coordination donor groups [160,161].

Recently, Yaghi and co-workers have synthesized a unique example of an imine-based 3D MCOF built from mononuclear cobalt(II) complexes with perpendicularly oriented aminophenyl-substituted PDI ligands as nodes of the woven framework, as depicted in Figure 18 [161]. The imine reaction synthesis not only facilitates the control of nucleation and crystal growth of the cobalt(II)-based woven MCOF, leading to uniform nanocrystals through microwave-assisted reactions (Figure 18a), but also allows for the straightforward

preparation of oriented thin films of 190 nm thickness on silicon substrates (Figure 18b). This unique class of woven MCOFs, comprising arrays of weakly interacting (“entangled”) and potentially switchable Co^{II} SCO-SIMs exhibiting sufficiently long quantum decoherence relaxation times, would offer an excellent opportunity to test them as prototypes of multiple qubit arrays for the construction of molecular logic systems, like spin quantum processors (SQPs).

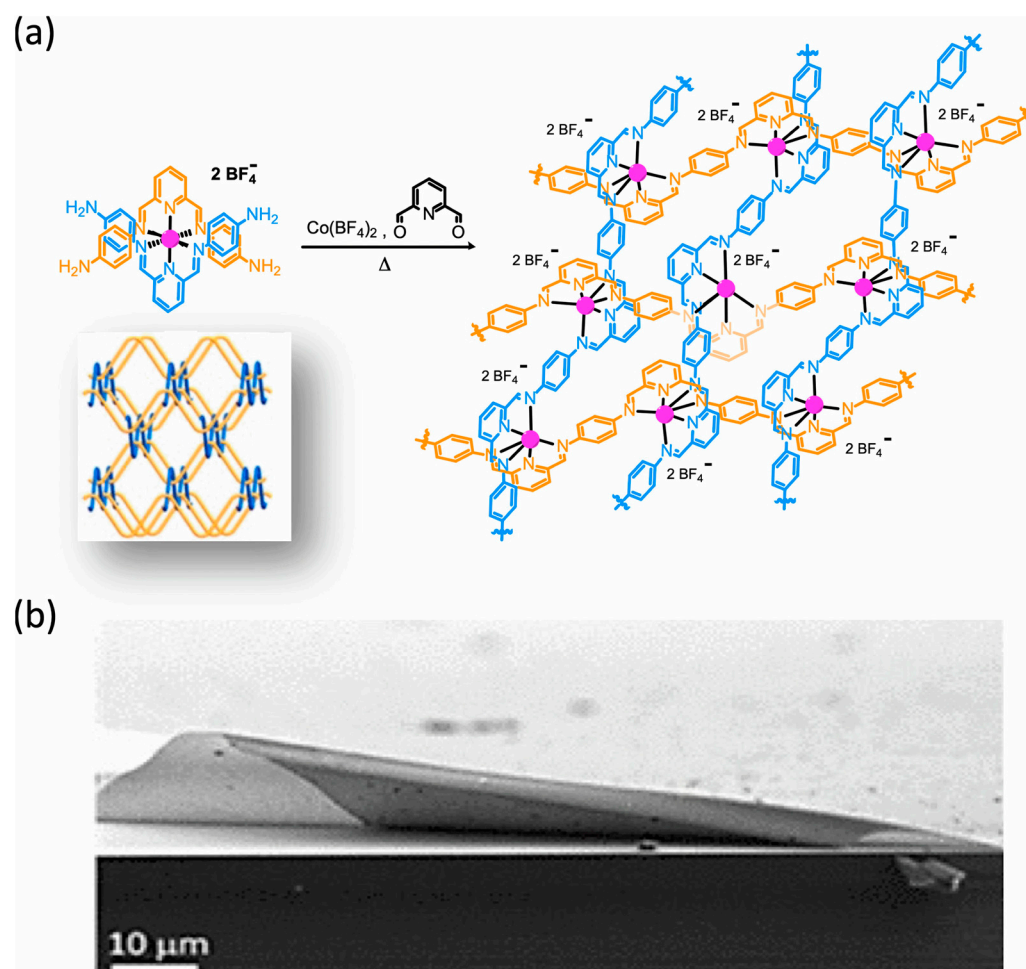


Figure 18. (a) An illustration of the 3D MCOF of diamond topology built from mononuclear cobalt(II) SCO-SIM complexes with phenylamine-substituted PDI ligands as nodes of the woven-like framework (see boxed structure) as a prototype of the molecular spin quantum processor. (b) A microphotograph of the oriented MCOF thin film showing high uniformity and small thickness. Adapted with permission from Ref. [161].

3. Conclusions and Outlook

“Every adventure requires a first step.” While this may sound cliché, it holds, particularly in science. The results gathered in this perspective review mark the initial steps of our research group in exploring multifunctional and multiresponsive magnetic devices based on spin-crossover molecular nanomagnets within the emerging fields of molecular spintronics and quantum computing. Although the search for some relationship (synergy) between the SCO and SIM properties is a challenging task, given the different temperature regions for each phenomenon, other alternatives exist that we explored along this family of cobalt(II)-TERPY and PDI SCO-SIM complexes. Hence, both SCO and SIM behaviors are sensible to other stimuli besides temperature, whether chemical (pH or analytes) or physical (light or electron flow), which allow the control of the spin state and spin relaxation dynamics simultaneously so that a spin modulation of the spin relaxation dynamics is

made possible. These results are also a key motivation for us to continue pursuing this challenging multidisciplinary research project where SCO and SIMs converge with redox and photophysical or photochemical properties. Indeed, most proposals concerning the scaling and addressing of spin-crossover cobalt(II) molecular nanomagnets as prototypes of single-molecule quantum spintronics and quantum computing devices feel more like daydreams or aspirations than tangible achievements. In the coming years, we aim to turn some of these dream worlds into reality, particularly in the physical realization of quantum information processing. In this respect, this perspective review serves as a message in a bottle for materials scientists with large expertise in manipulating and measuring single-molecule electron transport properties and those skilled in processing and addressing molecules on different supports, as well as for theoretical physicists who may find our work relevant for conceptualizing and scaling molecules as spin quantum bits in future quantum computers.

4. Epilog

“There is plenty of room at the bottom”. With all due respect, we would like to offer our own interpretation of Richard Feynman’s famous phrase, reflecting our perspective on the opportunities presented in this review. Our intention is not to undermine the original meaning of his invaluable insights, which have inspired numerous fields within Molecular Sciences, but rather to share the additional reflections that this statement evokes for us.

Molecular Sciences have indeed come a long way, and the remarkable advancements in this area have led us to a heightened awareness of its potential. It is widely acknowledged that nanoscience and nanotechnology have only scratched the surface of what is possible. These fields are highly competitive and evolve rapidly, often leading to a focus on the most significant or recent findings—the “top of the tip”. In this pursuit, many valuable results are overlooked simply because they were reported “too early”. Consequently, a lack of knowledge and appropriate techniques at the time has resulted in a wealth of findings being lost to scientific obscurity, which we refer to as “the bottom”. These results are still waiting for new, enthusiastic scientists to recognize their worth and recontextualize them with the current understanding and advanced technologies. This indicates that there is indeed plenty of room at the bottom.

We have thus realized that a new multifunctional system does not always need to arise from developing novel properties. Instead, by looking into “the bottom”, new materials may be created from creative designs that combine several well-known properties, establishing synergies between them. In this perspective review, we embraced the simple (but not effortless) idea of using two $\text{Co}^{\text{II}}\text{N}_6$ platforms with TERPY- and related PDI-type ligands, known for decades, to successfully obtain a new chemical library of spin-crossover molecular nanomagnets. Their chemical modulation and switchable behavior concerning both spin-crossover and the slow relaxation of magnetization phenomena illustrate the whole potential of this new class of multifunctional and multiresponsive magnetic molecules in molecular spintronics and quantum computing.

Author Contributions: This manuscript was written with the contributions of all authors. All authors have read and agreed to the published version of the manuscript.

Funding: This work was supported by the Spanish MINECO (Projects PID2019-109735GB-I00 and Unidad de Excelencia María de Maeztu CEX2019-000919-M) and the Generalitat Valenciana (AICO/2020/183 and AICO/2021/295). R. R. thanks the Generalitat Valenciana and CAPES/BRASIL for the doctoral (GRISOLIAP/2017/057) and postdoctoral (88887.798611/2022-00) grants.

Conflicts of Interest: The authors declare no conflicts of interest.

List of Abbreviations: AQ, anthraquinone; BEPYDMP, *N,N'*-bis(1-pyridin-2-ylethylidene)-2,2-dimethylpropane-1,3-diamine; BPYCA, 2,2'-bipyridine-4,4'-dicarboxamide; BPZ, dihydrobis(1-pyrazolyl)borate; CISS, chiral-induced spin-selectivity; CMOS, complementary metal-oxide-semiconductor; CNM, carbon nanomaterial; COF, covalent organic framework; DMPHEN, 2,9-dimethyl-1-10-phenanthroline; DFT, density functional theory; DPZBPY, 3,5-bis(pyrazol-1-yl)-4,4'-

bipyridine; DPZPY, 2,6-bis(pyrazol-1-yl)pyridine; EDX, energy-dispersive X-ray; EFE-SQT, electric field-effect spin quantum transistor; FET, field-effect transistor; FR, fast relaxation; GMR, giant magnetoresistance; HBDMPZ, hydrotris(3-5-dimethylpyrazole)borate; HS, high-spin; JT, Jahn-Teller; LB, Langmuir-Blodgett; LD-LISC, ligand-driven light-induced spin change; LED, light-emitting diode; LIESST, light-induced excited spin-state trapping; LMCT, ligand-to-metal charge transfer; LS, low-spin; MCOF, metal-covalent organic framework; MFE-SQT, magnetic field-effect spin quantum transistor; MLCT, metal-to-ligand charge transfer; MM, molecular magnetism; MNT, maleonitriledithiolate; MOF, metal-organic framework; PC, phthalocyanine; PDI, 2,6-pyridinediimine; QC, quantum coherence; QG, quantum gate; QIP, quantum information processing; QTM, quantum tunneling of magnetization; qubit, quantum bit; SAL, salicylaldehyde; S-BPP, (S)-(4-([2,6-(dipyrzolo-1-yl)pyrid-4-yl]ethynyl)phenyl)ethanethioate; SBU, secondary building unit; SCO, spin-crossover; SC-SC, single-crystal-to-single-crystal; SIM, single-ion magnet; SMM, single-molecule magnet; SMS, single-molecule spintronics; SOC, spin-orbit coupling; SQP, spin quantum processor; STM, scanning tunneling microscope; SQF, spin quantum filter; SQV, spin quantum valve; SR, slow relaxation; SWCNT, single-walled carbon nanotube; TERPY, 2,2':6',2'-terpyridine; TMC, 1,4,7,10-tetramethyl-1,4,7,10-tetraazacyclododecane; TMMPBA, *N,N'*-2,4,6-trimethyl-1,3-phenylenebis(oxamate); TZPY, 3-(2-pyridyl)[1-3]triazolo [1,5-a]pyridine; and UV, ultraviolet.

References

1. Moore, G.E. Cramming more components onto integrated circuits. *Electron. Mag.* **1965**, *38*, 114–117. [\[CrossRef\]](#)
2. Feynman, R.P. There's plenty of room at the bottom: An invitation to enter a new field of physics. *Eng. Sci.* **1960**, *23*, 22–36.
3. Baibich, M.N.; Broto, J.M.; Fert, A.; Nguyen Van Dau, F.; Petroff, F.; Etienne, P.; Creuzet, G.; Friederich, A.; Chazelas, J. Giant magnetoresistance of (001)Fe/(001)Cr magnetic superlattices. *Phys. Rev. Lett.* **1988**, *61*, 2472–2475. [\[CrossRef\]](#) [\[PubMed\]](#)
4. Binash, G.; Grünberg, P.; Saurenbach, F.; Zinn, W. Enhanced magnetoresistance in layered magnetic structures with antiferromagnetic interlayer exchange. *Phys. Rev. B* **1989**, *39*, 4828–4830. [\[CrossRef\]](#)
5. Awschalom, D.D.; Bassett, L.C.; Dzurak, A.S.; Hu, E.L.; Petta, J.R. Quantum spintronics: Engineering and manipulating atom-like spins in semiconductors. *Science* **2013**, *339*, 1174–1179. [\[CrossRef\]](#)
6. Arute, F.; Arya, K.; Babbush, R.; Bacon, D.; Bardin, J.C.; Barends, R.; Biswas, R.; Boixo, S.; Brandao, F.G.S.L.; Buell, D.A.; et al. Quantum supremacy using a programmable superconducting processor. *Nature* **2019**, *574*, 505–510. [\[CrossRef\]](#) [\[PubMed\]](#)
7. Zhong, H.-S.; Wang, H.; Deng, Y.-H.; Chen, M.-C.; Peng, L.-C.; Luo, Y.-H.; Qin, J.; Wu, D.; Ding, X.; Hu, P.; et al. Quantum computational advantage using photons. *Science* **2020**, *370*, 1460–1463. [\[CrossRef\]](#) [\[PubMed\]](#)
8. Peng, L.-C.; Wu, D.; Zhong, H.-S.; Luo, Y.-H.; Li, Y.; Hu, Y.; Jiang, X.; Chen, M.-C.; Li, L.; Liu, N.-L.; et al. Cloning of quantum entanglement. *Phys. Rev. Lett.* **2020**, *125*, 210502. [\[CrossRef\]](#)
9. Coronado, E. Molecular magnetism: From chemical design to spin control in molecules, materials and devices. *Nat. Rev. Mater.* **2020**, *5*, 87–104. [\[CrossRef\]](#)
10. Fert, A. Nobel lecture: Origin, development, and future of spintronics. *Rev. Mod. Phys.* **2008**, *8*, 1517–1530. [\[CrossRef\]](#)
11. Shor, P.W. Algorithms for quantum computation: Discrete logarithms and factoring. In Proceedings of the 35th Annual Symposium on Foundations of Computer Science, Santa Fe, NM, USA, 20–22 November 1994; Goldwasser, S., Ed.; IEEE Computer Society Press: Los Alamitos, CA, USA, 1994; pp. 124–134.
12. Grover, L.K. Quantum computers can search arbitrarily large databases by a single query. *Phys. Rev. Lett.* **1997**, *79*, 4709–4712. [\[CrossRef\]](#)
13. Kloeffel, C.; Loss, D. Prospects for spin-based quantum computing in quantum dots. *Annu. Rev. Condens. Matter Phys.* **2013**, *4*, 51–81. [\[CrossRef\]](#)
14. Sanvito, S. Molecular spintronics. *Chem. Soc. Rev.* **2011**, *40*, 3336–3355. [\[CrossRef\]](#)
15. Sanvito, S. Injecting and controlling spins in organic materials. *J. Mater. Chem.* **2007**, *17*, 4455–4459. [\[CrossRef\]](#)
16. Affronte, M.; Troiani, F.; Ghirri, A.; Candini, A.; Evangelisti, M.; Corradini, V.; Carretta, S.; Santini, P.; Amoretti, G.; Tuna, F.; et al. Single molecule magnets for quantum computation. *J. Phys. D Appl. Phys.* **2007**, *40*, 2999–3004. [\[CrossRef\]](#)
17. Bogani, L.; Wernsdorfer, W. Molecular spintronics using single-molecule magnets. *Nat. Mater.* **2008**, *7*, 179–186. [\[CrossRef\]](#) [\[PubMed\]](#)
18. Winpenny, R.E.P. Quantum information processing using molecular nanomagnets as qubits. *Angew. Chem. Int. Ed.* **2008**, *47*, 7992–7994. [\[CrossRef\]](#)
19. Lehmann, J.; Gaita-Ariño, A.; Coronado, E.; Loss, D. Quantum computing with molecular spin systems. *J. Mater. Chem.* **2009**, *19*, 1672–1677. [\[CrossRef\]](#)
20. Stamp, P.C.E.; Gaita-Ariño, A. Spin-based quantum computers made by chemistry: Hows and whys. *J. Mater. Chem.* **2009**, *19*, 1718–1730. [\[CrossRef\]](#)
21. Affronte, M. Molecular nanomagnets for information technologies. *J. Mater. Chem.* **2009**, *19*, 1731–1737. [\[CrossRef\]](#)
22. Ardavan, A.; Blundell, S.J. Storing quantum information in chemically engineered nanoscale magnets. *J. Mater. Chem.* **2009**, *19*, 1754–1760. [\[CrossRef\]](#)

23. Dei, A.; Gatteschi, D. Molecular (nano)magnets as test grounds of quantum mechanics. *Angew. Chem. Int. Ed.* **2011**, *50*, 11852–11858. [[CrossRef](#)]
24. Timco, G.A.; Faust, T.B.; Tuna, F.; Winpenny, R.E.P. Linking heterometallic rings for quantum information processing and amusement. *Chem. Soc. Rev.* **2011**, *40*, 3067–3075. [[CrossRef](#)]
25. Troiani, F.; Affronte, M. Molecular spins for quantum information technologies. *Chem. Soc. Rev.* **2011**, *40*, 3119–3129. [[CrossRef](#)]
26. Aromí, G.; Aguilà, D.; Gamez, P.; Luis, F.; Roubeau, O. Design of magnetic coordination complexes for quantum computing. *Chem. Soc. Rev.* **2012**, *41*, 537–546. [[CrossRef](#)] [[PubMed](#)]
27. Ghirri, A.; Troiani, F.; Affronte, M. Quantum computation with molecular nanomagnets: Achievements, challenges, and new trends. *Struct. Bond.* **2015**, *164*, 383–430.
28. Sessoli, R. Toward the quantum computer: Magnetic molecules back in the race. *ACS Cent. Sci.* **2015**, *1*, 473–474. [[CrossRef](#)]
29. Gaita-Ariño, A.; Luis, F.; Hill, S.; Coronado, E. Molecular spins for quantum computation. *Nat. Chem.* **2019**, *11*, 301–309. [[CrossRef](#)]
30. Figgins, P.E.; Busch, D.H. Complexes of iron(II), cobalt(II) and nickel(II) with biacetyl-bis-methylimine, 2-pyridinal-methylimine and 2,6-pyridindial-bis-methylimine. *J. Am. Chem. Soc.* **1960**, *82*, 820–824. [[CrossRef](#)]
31. Goodwin, H.A. Spin transitions in six-coordinate iron(II) complexes. *Coord. Chem. Rev.* **1976**, *18*, 293–325. [[CrossRef](#)]
32. Gütlich, P. Spin crossover in iron(II) complexes. *Struct. Bond.* **1981**, *44*, 83–195.
33. König, E.; Ritter, G.; Kulshreshtha, S.K. The nature of spin-state transitions in solid complexes of iron(II) and the interpretation of some associated phenomena. *Chem. Rev.* **1985**, *85*, 219–234. [[CrossRef](#)]
34. Boillot, M.L.; Sour, A.; Delhaes, P.; Mingotaud, C.; Soyer, H. A photomagnetic effect for controlling spin states of iron(II) complexes in molecular materials. *Coord. Chem. Rev.* **1999**, *190–192*, 47–59. [[CrossRef](#)]
35. Krivokapic, I.; Zerara, M.; Daku, M.L.; Vargas, A.; Enachescu, C.; Ambrus, C.; Tregenna-Piggott, P.; Amstutz, N.; Krausz, E.; Hauser, A. Spin-crossover in cobalt(II) imine complexes. *Coord. Chem. Rev.* **2007**, *251*, 364–378. [[CrossRef](#)]
36. Real, J.A.; Gaspar, A.B.; Muñoz, M.C. Thermal, pressure and light switchable spin-crossover materials. *Dalton Trans.* **2005**, 2062–2079. [[CrossRef](#)] [[PubMed](#)]
37. Bousseksou, A.; Molnár, G.; Salmon, L.; Nicolazzi, W. Molecular spin crossover phenomenon: Recent achievements and prospects. *Chem. Soc. Rev.* **2011**, *40*, 3313–3335. [[CrossRef](#)] [[PubMed](#)]
38. Ruiz, E. Charge transport properties of spin crossover systems. *Phys. Chem. Chem. Phys.* **2014**, *16*, 14–22. [[CrossRef](#)] [[PubMed](#)]
39. Bertoni, R.; Cammarata, M.; Lorenc, M.; Matar, S.F.; Matar, J.-F.; Létard, J.F.; Lemke, E.; Collet, H.T. Ultrafast light-induced spin-state trapping photophysics investigated in Fe(phen)₂(NCS)₂ spin-crossover crystal. *Acc. Chem. Res.* **2015**, *48*, 774–781. [[CrossRef](#)]
40. Harding, D.J.; Harding, P.; Phonsri, W. Spin crossover in iron(II) complexes. *Coord. Chem. Rev.* **2016**, *313*, 38–61. [[CrossRef](#)]
41. Khusniyarov, M.M. How to switch spin-crossover metal complexes at constant room temperature. *Chem. Eur. J.* **2016**, *22*, 15178–15191. [[CrossRef](#)]
42. Halcrow, M.A. Structure: Function relationships in molecular spin-crossover complexes. *Chem. Soc. Rev.* **2011**, *40*, 4119–4142. [[CrossRef](#)] [[PubMed](#)]
43. Halcrow, M.A. Spin-crossover compounds with wide thermal hysteresis. *Chem. Lett.* **2014**, *43*, 1178–1188. [[CrossRef](#)]
44. Halcrow, M.A. The effect of ligand design on metal ion spin state—Lessons from spin crossover complexes. *Crystals* **2016**, *6*, 58. [[CrossRef](#)]
45. Mallah, T.; Cavallini, M. Surfaces, thin films and patterning of spin crossover compounds. *C. R. Chimie* **2018**, *21*, 1270–1286. [[CrossRef](#)]
46. Molnár, G.; Rat, S.; Salmon, L.; Nicolazzi, W.; Bousseksou, A. Spin crossover nanomaterials: From fundamental concepts to devices. *Adv. Mater.* **2018**, *30*, 17003862. [[CrossRef](#)]
47. Molnár, G.; Mikolasek, M.; Ridier, K.; Fahs, A.; Nicolazzi, W.; Bousseksou, A. Molecular spin crossover materials: Review of the lattice dynamical properties. *Ann. Phys.* **2019**, *531*, 1900076. [[CrossRef](#)]
48. Cirera, J.; Ruiz, E.; Alvarez, S.; Neese, F.; Kortus, J. How to build molecules with large magnetic anisotropy. *Chem. Eur. J.* **2009**, *15*, 4078–4087.
49. Neese, F.; Pantazis, D.A. What is not required to make a single molecule magnet. *Faraday Discuss.* **2011**, *148*, 229–238. [[PubMed](#)]
50. Atanasov, M.; Aravena, D.; Suturina, E.; Bill, E.; Maganas, D.; Neese, F. First principles approach to the electronic structure, magnetic anisotropy and spin relaxation in mononuclear 3d-transition metal single molecule magnets. *Coord. Chem. Rev.* **2015**, *289–290*, 177–214.
51. Gomez-Coca, S.; Aravena, D.; Morales, R.; Ruiz, E. Large magnetic anisotropy in mononuclear metal complexes. *Coord. Chem. Rev.* **2015**, *289–290*, 379–392. [[CrossRef](#)]
52. Chibotaru, L.F. Theoretical understanding of anisotropy in molecular nanomagnets. *Struct. Bond.* **2015**, *164*, 185–229.
53. Craig, G.A.; Murrie, M. 3d Single-ion magnets. *Chem. Soc. Rev.* **2015**, *44*, 2135–2147. [[CrossRef](#)] [[PubMed](#)]
54. Frost, J.M.; Harriman, K.L.M.; Murugesu, M. The rise of 3-d single-ion magnets in molecular magnetism: Towards materials from molecules? *Chem. Sci.* **2016**, *7*, 2470–2491. [[CrossRef](#)]
55. Bar, A.K.; Pichon, C.; Sutter, J.-P. Magnetic anisotropy in two- to eight-coordinated transition-metal complexes: Recent developments in molecular magnetism. *Coord. Chem. Rev.* **2016**, *308*, 346–380. [[CrossRef](#)]
56. Meng, Y.-S.; Jiang, S.-D.; Wang, B.-W.; Gao, S. Understanding the magnetic anisotropy toward single-ion magnets. *Acc. Chem. Res.* **2016**, *49*, 2381–2389. [[CrossRef](#)]
57. Feng, M.; Tong, M.-L. Single-ion magnets from 3d to 5f: Developments and strategies. *Chem. Eur. J.* **2018**, *24*, 7574–7594. [[CrossRef](#)] [[PubMed](#)]

58. Moreno-Pineda, E.; Wernsdorfer, W. Measuring molecular magnets for quantum technologies. *Nat. Rev. Phys.* **2021**, *3*, 645–659. [[CrossRef](#)]
59. Zabala-Lekuona, A.; Seco, J.M.; Colacio, E. Single-molecule magnets: From Mn12-ac to dysprosium metallocenes. A travel in time. *Coord. Chem. Rev.* **2021**, *441*, 213984. [[CrossRef](#)]
60. Chilton, N.F. Molecular Magnetism. *Annu. Rev. Matter. Res.* **2022**, *52*, 79–101. [[CrossRef](#)]
61. Park, J.; Pasupathy, A.N.; Goldsmith, J.I.; Chang, C.; Yaish, Y.; Petta, J.R.; Rinkoski, M.; Sethna, J.P.; Abruña, H.D.; McEuen, P.L.; et al. Coulomb blockade and the kondo effect in single-atom transistors. *Nat. Mater.* **2002**, *417*, 722–725. [[CrossRef](#)] [[PubMed](#)]
62. Parks, J.J.; Champagne, A.R.; Costi, T.A.; Shum, W.W.; Pasupathy, A.N.; Neuscamman, E.; Flores-Torres, S.; Cornaglia, P.S.; Aligia, A.A.; Balseiro, C.A.; et al. Mechanical control of spin states in spin-1 molecules and the underscreened kondo effect. *Science* **2010**, *328*, 1370–1373. [[CrossRef](#)]
63. Meded, V.; Bagrets, A.; Fink, K.; Chandrasekar, R.; Ruben, M.; Evers, F.; Bernand-Mantel, A.; Seldenthuis, J.S.; Beukman, A.; van der Zant, H.S.J. Electrical control over the Fe(II) spin crossover in a single molecule: Theory and experiment. *Phys. Rev. B* **2011**, *83*, 245415. [[CrossRef](#)]
64. Harzmann, G.D.; Frisenda, R.; van der Zant, H.S.J.; Mayor, M. Single-molecules spin switch based on voltage-triggered distortion of the coordination sphere. *Angew. Chem. Int. Ed.* **2015**, *54*, 13425–13430. [[CrossRef](#)]
65. Devid, E.J.; Martinho, P.N.; Kamalakar, M.V.; Salitros, I.; Prendergast, Ú.; Dayen, J.-F.; Meded, V.; Lemma, T.; González-Pietro, R.; Evers, F.; et al. Spin transition in arrays of gold nanoparticles and spin crossover molecules. *ACS Nano* **2015**, *9*, 4486–4507. [[CrossRef](#)]
66. Aravena, D.; Ruiz, E. Coherent transport through spin-crossover single molecules. *J. Am. Chem. Soc.* **2012**, *134*, 777–779. [[CrossRef](#)]
67. Aragonès, A.C.; Aravena, D.; Cerdá, J.I.; Acís-Castillo, Z.; Li, H.; Real, J.A.; Sanz, F.; Hihath, J.; Ruiz, E.; Díez-Pérez, I. Large conductance switching in a single-molecule device through room temperature spin-dependent transport. *Nano Lett.* **2016**, *16*, 218–226. [[CrossRef](#)] [[PubMed](#)]
68. Katsnelson, M.I. Graphene: Carbon in two dimensions. *Mater. Today* **2007**, *10*, 20–27. [[CrossRef](#)]
69. Konstantinov, N.; Tauzin, A.; Noubé, U.N.; Dragoe, D.; Kundys, B.; Majjad, H.; Brosseau, A.; Lenertz, M.; Singh, A.; Berciaud, S.; et al. Electrical read-out of light-induced spin transition in thin film spin crossover/graphene heterostructures. *J. Mater. Chem. C* **2021**, *9*, 2712–2720. [[CrossRef](#)]
70. Lee, C.W.; Kim, O.Y.; Lee, J.Y. Organic materials for organic electronic devices. *J. Ind. Eng. Chem.* **2014**, *20*, 1198–1208. [[CrossRef](#)]
71. Komeda, T.; Isshiki, H.; Liu, J.; Zhang, Y.-F.; Lorente, N.; Katoh, K.; Breedlove, B.K.; Yamashita, M. Observation and electric current control of a local spin in a single-molecule magnet. *Nat. Commun.* **2011**, *2*, 217–223. [[CrossRef](#)] [[PubMed](#)]
72. Kyatskaya, S.; Galán-Mascarós, J.R.; Bogani, L.; Hennrich, F.; Kappes, M.; Wernsdorfer, W.; Ruben, M. Anchoring of rare-earth-based single-molecule magnets on single-walled carbon nanotubes. *J. Am. Chem. Soc.* **2009**, *131*, 15143–15151. [[CrossRef](#)] [[PubMed](#)]
73. Urdampilleta, M.; Klyatskaya, S.; Cleuziou, J.-P.; Ruben, M.; Wernsdorfer, W. Supramolecular spin valves. *Nat. Mater.* **2011**, *10*, 502–506. [[CrossRef](#)] [[PubMed](#)]
74. Muñoz, M.C.; Real, J.A. Thermo-, piezo-, photo- and chemo-switchable spin crossover iron(II)-metallocyanate based coordination polymers. *Coord. Chem. Rev.* **2011**, *255*, 2068–2093. [[CrossRef](#)]
75. Goodwin, H.A. Spin crossover in cobalt(II) systems. *Top. Curr. Chem.* **2004**, *234*, 23–47.
76. Cowan, M.G.; Olguín, J.; Narayanaswamy, S.; Tallon, J.L.; Brooker, S. Reversible switching of a cobalt complex by thermal, pressure, and electrochemical stimuli: Abrupt, complete, hysteretic spin crossover. *J. Am. Chem. Soc.* **2012**, *134*, 2892–2894. [[CrossRef](#)] [[PubMed](#)]
77. Kahn, O. *Molecular Magnetism*; VCH Publishers: New York, NY, USA, 1993.
78. Ishikawa, N.; Sugita, M.; Ishikawa, T.; Koshihara, S.Y.; Kaizu, Y. Lanthanide double-decker complexes functioning as magnets at the single-molecular level. *J. Am. Chem. Soc.* **2003**, *125*, 8694–8695. [[CrossRef](#)] [[PubMed](#)]
79. Ishikawa, N.; Sugita, M.; Okubo, T.; Tanaka, N.; Lino, T.; Kaizu, Y. Determination of ligand-field parameters and f-electronic structures of double-decker bis(phthalocyaninato)lanthanide complexes. *Inorg. Chem.* **2003**, *42*, 2440–2446. [[CrossRef](#)] [[PubMed](#)]
80. Ishikawa, N.; Sugita, M.; Ishikawa, T.; Koshihara, S.-Y.; Kaizu, Y. Mononuclear lanthanide complexes with a long magnetisation relaxation time at high temperatures: A new category of magnets at the single-molecular level. *J. Phys. Chem. B* **2004**, *108*, 11265–11271. [[CrossRef](#)]
81. Vallejo, J.; Castro, I.; Ruiz-García, R.; Cano, J.; Julve, M.; Lloret, F.; De Munno, G.; Wernsdorfer, W.; Pardo, E. Field-induced slow magnetic relaxation in a six-coordinate mononuclear cobalt(II) complex with a positive anisotropy. *J. Am. Chem. Soc.* **2012**, *134*, 15704–15707. [[CrossRef](#)] [[PubMed](#)]
82. Gaspar, A.B.; Ksenofontov, V.; Seredyuk, M.; Gutlich, P. Multifunctionality in spin crossover materials. *Coord. Chem. Rev.* **2005**, *249*, 2661–2676. [[CrossRef](#)]
83. Bousseksou, A.; Molnár, G.; Demont, P.; Menegotto, J. Observation of a thermal hysteresis loop in the dielectric constant of spin crossover complexes: Towards molecular memory devices. *J. Mater. Chem.* **2003**, *13*, 2069–2071. [[CrossRef](#)]
84. Kumar, K.S.; Ruben, M. Emerging trends in spin crossover (SCO) based functional materials and devices. *Coord. Chem. Rev.* **2017**, *346*, 176–205. [[CrossRef](#)]
85. Gutlich, P.; Hauser, A. Thermal and light-induced spin crossover in iron(II) complexes. *Coord. Chem. Rev.* **1990**, *97*, 1–22. [[CrossRef](#)]

86. Hayami, S.; Komatsu, Y.; Shimizu, T.; Kamihata, H.; Lee, Y.H. Spin-crossover in cobalt(II) compounds containing terpyridine and its derivatives. *Coord. Chem. Rev.* **2011**, *255*, 1981–1990. [[CrossRef](#)]
87. Galet, A.; Gaspar, A.B.; Muñoz, M.C.; Real, J.A. Influence of the counterion and the solvent molecules in the spin crossover system $[\text{Co}(\text{4-terpyridone})_2]X_p \cdot n\text{H}_2\text{O}$. *Inorg. Chem.* **2006**, *45*, 4413–4422. [[CrossRef](#)]
88. Murrie, M. Cobalt(II) single-molecule magnets. *Chem. Soc. Rev.* **2010**, *39*, 1986–1995. [[CrossRef](#)]
89. Ding, Y.-S.; Deng, Y.-F.; Zheng, Y.-Z. The rise of single-ion magnets as spin qubits. *Magnetochemistry* **2016**, *2*, 40. [[CrossRef](#)]
90. Zadrozny, J.M.; Long, J.R. Slow magnetic relaxation at zero field in the tetrahedral complex $[\text{Co}(\text{SPh})_4]^{2-}$. *J. Am. Chem. Soc.* **2011**, *133*, 20732–20734. [[CrossRef](#)] [[PubMed](#)]
91. Lloret, F.; Julve, M.; Cano, J.; Ruiz-García, R.; Pardo, E. Magnetic properties of six-coordinated high-spin cobalt(II) complexes: Theoretical background and its application. *Inorg. Chim. Acta* **2008**, *361*, 3432–3445. [[CrossRef](#)]
92. Herchel, R.; Váhovská, L.; Potocnák, I.; Trávníček, Z. Slow magnetic relaxation in octahedral cobalt(II) field-induced single-ion magnet with positive axial and large rhombic anisotropy. *Inorg. Chem.* **2014**, *53*, 5896–5898. [[CrossRef](#)] [[PubMed](#)]
93. Roy, S.; Oyarzabal, I.; Vallejo, J.; Cano, J.; Colacio, E.; Bauza, A.; Frontera, A.; Kirillov, A.M.; Drew, M.G.B.; Das, S. Two polymorphic forms of a six-coordinate mononuclear cobalt(II) complex with easy-plane anisotropy: Structural features, theoretical calculations, and field-induced slow relaxation of the magnetisation. *Inorg. Chem.* **2016**, *55*, 8502–8513. [[CrossRef](#)] [[PubMed](#)]
94. Ding, Z.-Y.; Meng, Y.-S.; Xiao, Y.; Zhang, Y.-Q.; Zhu, Y.-Y.; Gao, S. Probing the influence of molecular symmetry on the magnetic anisotropy of octahedral cobalt(II) complexes. *Inorg. Chem. Front.* **2017**, *4*, 1909–1916. [[CrossRef](#)]
95. Wu, Y.; Tian, D.; Ferrando-Soria, J.; Cano, J.; Yin, L.; Ouyang, Z.; Wang, Z.; Luo, S.; Liu, X.; Pardo, E. Modulation of the magnetic anisotropy of octahedral cobalt(II) single-ion magnets by fine-tuning the axial coordination microenvironment. *Inorg. Chem. Front.* **2019**, *6*, 848–856. [[CrossRef](#)]
96. Cen, P.; Yuan, W.; Tan, M.; Chen, B.; Song, W.; Wang, Z.; Liu, X. Field-induced slow magnetic relaxation in an octahedral high-spin Co(II) complex. *Inorg. Chem. Commun.* **2019**, *99*, 195–198. [[CrossRef](#)]
97. Palion-Gazda, J.; Machura, B.; Kruszynski, R.; Grancha, T.; Moliner, N.; Lloret, F.; Julve, M. Spin crossover in double salts containing six- and four-coordinate cobalt(II) ions. *Inorg. Chem.* **2017**, *56*, 6281–6296. [[CrossRef](#)] [[PubMed](#)]
98. Shao, D.; Deng, L.-D.; Shi, L.; Wu, D.-Q.; Wei, X.-Q.; Yang, S.-R.; Wang, X.-Y. Slow magnetic relaxation and spin crossover behaviour in a bicomponent ion-pair cobalt(II) complex. *Eur. J. Inorg. Chem.* **2017**, *2017*, 3862–3867. [[CrossRef](#)]
99. Cui, H.-H.; Wang, J.; Chen, X.-T.; Xue, Z.-L. Slow magnetic relaxation in five-coordinate spin-crossover cobalt(II) complexes. *Chem. Commun.* **2017**, *53*, 9304–9307. [[CrossRef](#)] [[PubMed](#)]
100. Chen, L.; Song, J.; Zhao, W.; Yi, G.; Zhou, Z.; Yuan, A.; Song, Y.; Wang, Z.; Ouyang, Z.-W. A mononuclear five-coordinate Co(II) single molecule magnet with a spin crossover between the $S = 1/2$ and $3/2$ states. *Dalton Trans.* **2018**, *47*, 16596–16602. [[CrossRef](#)]
101. Xu, M.-X.; Liu, Z.; Dong, B.-W.; Cui, H.-H.; Wang, Y.-X.; Su, J.; Wang, Z.; Song, Y.; Chen, X.-T.; Jiang, S.-D.; et al. Single-crystal study of a low spin Co(II) molecular qubit: Observation of anisotropic rabi cycles. *Inorg. Chem.* **2019**, *58*, 2330–2335. [[CrossRef](#)] [[PubMed](#)]
102. Shao, D.; Shi, L.; Yin, J.; Wang, B.-L.; Wang, Z.-X.; Zhang, Y.-Q.; Wang, X.-Y. Reversible on-off switching of both spin crossover and single-molecule magnet behaviours via a crystal-to-crystal transformation. *Chem. Sci.* **2018**, *9*, 7986–7991. [[CrossRef](#)] [[PubMed](#)]
103. Kobayashi, F.; Komatsumaru, Y.; Akiyoshi, R.; Nakamura, M.; Zhang, Y.; Lindoy, L.F.; Hayami, S. Water molecule-induced reversible magnetic switching in a bis-terpyridine cobalt(II) complex exhibiting coexistence of spin crossover and orbital transition behaviors. *Inorg. Chem.* **2020**, *59*, 16843–16852. [[CrossRef](#)] [[PubMed](#)]
104. Rabelo, R.; Toma, L.; Moliner, N.; Julve, M.; Lloret, F.; Pasán, J.; Ruiz-Pérez, C.; Ruiz-García, R.; Cano, J. Electro-switching of the single-molecule magnet behaviour in an octahedral spin crossover cobalt(II) complex with a redox-active pyridinediimine ligand. *Chem. Commun.* **2020**, *56*, 12242–12245. [[CrossRef](#)]
105. Rabelo, R.; Toma, L.; Moliner, N.; Julve, M.; Lloret, F.; Inclán, M.; García-España, E.; Pasán, J.; Ruiz-García, R.; Cano, J. pH-Switching of the luminescent, redox, and magnetic properties in a spin crossover cobalt(II) molecular nanomagnet. *Chem. Sci.* **2023**, *14*, 8850. [[CrossRef](#)] [[PubMed](#)]
106. Rabelo, R.; Toma, L.; Julve, M.; Lloret, F.; Pasán, J.; Cangussu, D.; Ruiz-García, R.; Cano, J. How the spin state tunes the slow magnetic relaxation field dependence in spin crossover cobalt(II) complexes. *Dalton Trans.* **2024**, *53*, 5507–5520. [[CrossRef](#)] [[PubMed](#)]
107. Rabelo, R.; Toma, L.; Julve, M.; Lloret, F.; Pasán, J.; Cangussu, D.; Ruiz-García, R.; Cano, J. Multi-electron transfer and field-induced slow magnetic relaxation in spin crossover cobalt(II) complexes: Structure-function correlations. *Inorg. Chem. Front.* **2024**, *11*, 6028–6043. [[CrossRef](#)]
108. Canton, S.E.; Biednov, M.; Pápai, M.; Lima, F.A.; Choi, T.-K.; Otte, F.; Jiang, Y.; Frankenberger, P.; Knoll, M.; Zalden, P.; et al. Ultrafast Jahn-Teller photoswitching in cobalt single-ion magnets. *Adv. Sci.* **2023**, *10*, 2206880. [[CrossRef](#)]
109. Urtizberea, A.; Roubeau, O. Switchable slow relaxation of magnetization in the native low temperature phase of a cooperative spin crossover compound. *Chem. Sci.* **2017**, *8*, 2290–2295. [[CrossRef](#)] [[PubMed](#)]
110. Feng, X.; Mathonière, C.; Jeon, I.-R.; Rouzières, M.; Ozarowski, A.; Aubrey, M.L.; Gonzalez, M.I.; Clérac, R.; Long, J.R. Tristability in a light-actuated single-molecule magnet. *J. Am. Chem. Soc.* **2013**, *135*, 15880–15884. [[CrossRef](#)]
111. Mathonière, C.; Lin, H.-J.; Siretanu, D.; Clérac, R.; Smith, J.M. Photoinduced single-molecule magnet properties in a four-coordinate iron(II) spin crossover complex. *J. Am. Chem. Soc.* **2013**, *135*, 19083–19086. [[CrossRef](#)] [[PubMed](#)]

112. Ferrando-Soria, J.; Vallejo, J.; Castellano, M.; Martínez-Lillo, J.; Pardo, E.; Cano, J.; Castro, I.; Lloret, F.; Ruiz-García, R.; Julve, M. Molecular magnetism, quo vadis? A historical perspective from a coordination chemist viewpoint. *Coord. Chem. Rev.* **2017**, *339*, 17–103. [[CrossRef](#)]
113. Ruben, M.; Rojo, J.; Romero-Salguero, F.J.; Uppadine, L.H.; Lehn, J.-M. Grid-type metal ion architectures: Functional metallo-supramolecular arrays. *Angew. Chem. Int. Ed.* **2004**, *43*, 3644–3662. [[CrossRef](#)] [[PubMed](#)]
114. Moriuchi, T.; Hirao, T. Design and redox function of conjugated complexes with polyanilines or quinonediimines. *Acc. Chem. Res.* **2012**, *45*, 347–360. [[CrossRef](#)]
115. Mansoor, I.F.; Wozniak, D.I.; Wu, Y.; Lipke, M.C. A delocalized cobaltoviologen with seven reversibly accessible redox states and highly tunable electrochromic behaviour. *Chem. Commun.* **2020**, *56*, 13864–13867. [[CrossRef](#)] [[PubMed](#)]
116. Liu, Q.; Liu, X.; Shi, C.; Zhang, Y.; Feng, X.; Cheng, M.-L.; Su, S.; Gu, J. A copper-based layered coordination polymer: Synthesis, magnetic properties and electrochemical performance in supercapacitors. *Dalton Trans.* **2015**, *44*, 19175–19184. [[CrossRef](#)]
117. Zhang, Q.; Uchaker, E.; Candelaria, S.L.; Cao, G. Nanomaterials for energy conversion and storage. *Chem. Soc. Rev.* **2013**, *42*, 3127–3171. [[CrossRef](#)] [[PubMed](#)]
118. Durfee, W.S.; Pierpont, C.G. Complexes of quinone-functionalised chelating ligands for multiple electron/proton transfer reduction reactions. *Inorg. Chem.* **1993**, *32*, 493–494. [[CrossRef](#)]
119. Malwitz, J.; Alkire, N.; Durfee, W. Quinone-functionalized transition metal complexes for multi-electron transfer. the electrochemistry of a bis-naphthoquinone-functionalized schiff base Ni(II) complex. *J. Coord. Chem.* **2010**, *55*, 641–650. [[CrossRef](#)]
120. Roux, C.; Zarembowitch, J.; Gallois, B.; Granier, T.; Claude, R. Toward ligand-driven light-induced spin changing. influence of the configuration of 4-styrylpyridine (stpy) on the magnetic properties of Fe^{II}(stpy)₄(NCS)₂ complexes. Crystal Structures of the spin-crossover species Fe(*trans*-stpy)₄(NCS)₂ and of the high-spin species Fe(*cis*-stpy)₄(NCS)₂. *Inorg. Chem.* **1994**, *33*, 2273–2279.
121. Dietrich-Buchecker, C.O.; Sauvage, J.-P.; Kintzinger, J.-P. Une nouvelle famille de molécules: Les métallo-caténanes. *Tetrahedron Lett.* **1983**, *24*, 5095–5098. [[CrossRef](#)]
122. Mohr, B.; Sauvage, J.-P.; Grubbs, R.H.; Weck, M. High-yield synthesis of [2]catenanes by intramolecular ring-closing metathesis. *Angew. Chem. Int. Ed.* **1997**, *36*, 1308–1310. [[CrossRef](#)]
123. Hruby, J.; Vavrecková, S.; Masaryk, L.; Sojka, A.; Navarro-Giraldo, J.; Bartos, M.; Herchel, R.; Moncol, J.; Nemeč, I.; Neugebauer, P. Deposition of tetracoordinate Co(II) complex with chalcone ligands on graphene. *Molecules* **2020**, *25*, 5021. [[CrossRef](#)] [[PubMed](#)]
124. Hruby, J.; Dvořák, D.; Squillantini, L.; Mannini, M.; van Slageren, J.; Herchel, R.; Nemeč, I.; Neugebauer, P. Co(II)-based single-ion magnets with 1,1'-ferrocenediyl-bis(diphenylphosphine) metalloligands. *Dalton Trans.* **2020**, *49*, 11697–11707. [[CrossRef](#)] [[PubMed](#)]
125. Juráková, J.; Midlíková, J.D.; Hruby, J.; Kliuikov, A.; Santana, V.T.; Pavlik, J.; Moncol, J.; Cizmár, E.; Orlita, M.; Mohelsky, I.; et al. Pentacoordinate cobalt(II) single ion magnets with pendant alkyl chains: Shall we go for chloride or bromide? *Inorg. Chem. Front.* **2022**, *9*, 1179–1194. [[CrossRef](#)]
126. Juráková, J.; Fellner, O.F.; Schlittenhardt, S.; Vavrecková, S.; Nemeč, I.; Herchel, R.; Cizmár, E.; Santana, V.T.; Orlita, M.; Gentili, D.; et al. Neutral cobalt(II)-bis(benzimidazole)pyridine field-induced single-ion magnets for surface deposition. *Inorg. Chem. Front.* **2023**, *10*, 5406–5419. [[CrossRef](#)]
127. Navarro-Giraldo, J.; Hruby, J.; Vavrecková, S.; Fellner, O.F.; Havlicek, L.; Henry, D.; de Silva, S.; Herchel, R.; Bartos, M.; Salitros, I.; et al. Tetracoordinate Co(II) complexes with semi-coordination as stable single-ion magnets for deposition on graphene. *Phys. Chem. Chem. Phys.* **2023**, *25*, 29516–29530. [[CrossRef](#)]
128. García-López, V.; Giaconi, N.; Poggini, L.; Calbo, J.; Juhin, A.; Cortigiani, B.; Herrero-Martín, J.; Ortí, E.; Mannini, M.; Clemente-León, M.; et al. Spin-crossover grafted monolayer of a Co(II) terpyridine derivative functionalized with carboxylic acid groups. *Adv. Func. Mater.* **2023**, *33*, 2300351. [[CrossRef](#)]
129. Bloom, B.P.; Paltiel, Y.; Naaman, R.; Waldeck, D.H. Chiral Induced Spin Selectivity. *Chem. Rev.* **2024**, *124*, 1950–1991. [[CrossRef](#)] [[PubMed](#)]
130. Torres-Cavanillas, R.; Escorzia-Ariza, G.; Brotons-Alcázar, I.; Sanchis-Gual, R.; Mondal, P.C.; Rosaleny, L.E.; Giménez-Santamarina, S.; Sessolo, M.; Galbiati, M.; Tatay, S.; et al. Reinforced Room-Temperature Spin Filtering in Chiral Paramagnetic Metallopeptides. *J. Am. Chem. Soc.* **2020**, *142*, 17572–17580. [[CrossRef](#)] [[PubMed](#)]
131. Cardona-Serra, S.; Rosaleny, L.E.; Giménez-Santamarina, S.; Martínez-Gil, L.; Gaita-Ariño, A. Towards peptide-based tunable multistate memristive materials. *Phys. Chem. Chem. Phys.* **2021**, *23*, 1802–1810. [[CrossRef](#)] [[PubMed](#)]
132. Zdrozny, J.M.; Niklas, J.; Poluektov, O.G.; Freedman, D.E. Multiple quantum coherences form hyperfine transitions in a vanadium(IV) complex. *J. Am. Chem. Soc.* **2014**, *136*, 15841–15844. [[CrossRef](#)]
133. Zdrozny, J.M.; Freedman, D.E. Qubit control limited by spin-lattice relaxation in a nuclear spin-free iron(III) complex. *Inorg. Chem.* **2015**, *54*, 12027–12031. [[CrossRef](#)] [[PubMed](#)]
134. Fataftah, M.S.; Zdrozny, J.M.; Coste, S.C.; Graham, M.J.; Rogers, D.M.; Freedman, D.E. Employing forbidden transitions as qubits in a nuclear spin-free chromium complex. *J. Am. Chem. Soc.* **2016**, *138*, 1344–1348. [[CrossRef](#)]
135. Yu, C.J.; Graham, M.J.; Zdrozny, J.M.; Niklas, J.; Krzyaniak, M.; Wasielewski, M.R.; Poluektov, O.G.; Freedman, D.E. Long coherence times in nuclear spin-free vanadyl qubits. *J. Am. Chem. Soc.* **2016**, *138*, 14678–14685. [[CrossRef](#)]
136. Bader, K.; Dengler, D.; Lenz, S.; Endeward, B.; Jiang, S.-D.; Neugebauer, P.; van Slageren, J. Room temperature quantum coherence in a potential molecular qubit. *Nat. Commun.* **2014**, *5*, 5304–5308. [[CrossRef](#)]

137. Atzori, M.; Tesi, L.; Morra, E.; Chiesa, M.; Sorace, L.; Sessoli, R. Room-temperature quantum coherence and rabi oscillations in vanadyl phthalocyanine: Toward multifunctional molecular spin qubits. *J. Am. Chem. Soc.* **2016**, *138*, 2154–2157. [[CrossRef](#)]
138. Bader, K.; Winkler, M.; van Slageren, J. Tuning of molecular qubits: Very long coherence and spin–lattice relaxation times. *Chem. Commun.* **2016**, *52*, 3623–3626. [[CrossRef](#)]
139. Carbonell-Vilar, J.M. Estudio de Propiedades Magnéticas en Compuestos de Coordinación Multifuncionales. Ph.D. Thesis, Universitat de València, Valencia, Spain, 2021.
140. Rabelo, R. Spin Crossover Cobalt(II) Molecular Nanomagnets as Dynamic Molecular Systems. Ph.D. Thesis, Universitat de València, Valencia, Spain, 2022.
141. Soyer, H.; Mingotaud, C.; Boillot, M.L.; Delhaes, P. Spin crossover of a langmuir–blodgett film based on an amphiphilic iron(II) complex. *Langmuir* **1998**, *14*, 5890–5895. [[CrossRef](#)]
142. Soyer, H.; Mingotaud, C.; Boillot, M.L.; Delhaes, P. Spin-crossover complex stabilized on a formamide/water subphase. *Thin Solid Films* **1998**, *329*, 435–438. [[CrossRef](#)]
143. Luo, Y.-H.; Liu, Q.-L.; Yang, L.-J.; Sun, Y.; Wang, J.-W.; You, C.-Q.; Sun, B.-W. Magnetic observation of above room-temperature spin transition in vesicular nano-spheres. *J. Mater. Chem. C* **2016**, *4*, 8061–8069. [[CrossRef](#)]
144. Hayami, S.; Shige-yoshi, Y.; Akita, M.; Inoue, K.; Kato, K.; Osaka, K.; Takata, M.; Kawajiri, R.; Mitani, T.; Maeda, Y. Reverse spin transition triggered by a structural phase transition. *Angew. Chem. Int. Ed.* **2005**, *44*, 4899–4903. [[CrossRef](#)] [[PubMed](#)]
145. Kitagawa, S.; Kitaura, R.; Noro, S.I. Functional porous coordination polymers. *Angew. Chem. Int. Ed.* **2004**, *43*, 2334–2375. [[CrossRef](#)] [[PubMed](#)]
146. Kitagawa, S.; Matsuda, R. Chemistry of coordination space of porous coordination polymers. *Coord. Chem. Rev.* **2007**, *251*, 2490–2509. [[CrossRef](#)]
147. Férey, G.; Serre, C. Large breathing effects in three-dimensional porous hybrid matter: Facts, analyses, rules and consequences. *Chem. Soc. Rev.* **2009**, *38*, 1380–1399. [[CrossRef](#)] [[PubMed](#)]
148. Mon, M.; Bruno, R.; Ferrando-Soria, J.; Armentano, D.; Pardo, E. Metal–organic framework technologies for water remediation: Towards a sustainable ecosystem. *J. Mat. Chem. A* **2018**, *6*, 4912–4947. [[CrossRef](#)]
149. Viciano-Chumillas, M.; Mon, M.; Ferrando-Soria, J.; Corma, A.; Leyva-Pérez, A.; Armentano, D.; Pardo, E. Metal–organic frameworks as chemical nanoreactors: Synthesis and stabilisation of catalytically active metal species in confined spaces. *Acc. Chem. Res.* **2020**, *53*, 520–531. [[CrossRef](#)]
150. Ferrando-Soria, J.; Ruiz-García, R.; Cano, J.; Stiriba, S.-E.; Vallejo, J.; Castro, I.; Julve, M.; Lloret, F.; Amorós, P.; Pasán, J.; et al. Reversible solvatomagnetic switching in a spongelike manganese(II)–copper(II) 3D open framework with a pillared square/octagonal layer architecture. *Chem. Eur. J.* **2012**, *18*, 1608–1617. [[CrossRef](#)] [[PubMed](#)]
151. Abhervé, A.; Grancha, T.; Ferrando-Soria, J.; Clemente-León, M.; Coronado, E.; Waerenborgh, J.C.; Lloret, F.; Pardo, E. Spin-crossover complex encapsulation within a magnetic metal–organic framework. *Chem. Commun.* **2016**, *52*, 7360–7363. [[CrossRef](#)] [[PubMed](#)]
152. Mon, M.; Pascual-Álvarez, A.; Grancha, T.; Cano, J.; Ferrando-Soria, J.; Lloret, F.; Gascon, J.; Pasán, J.; Armentano, D.; Pardo, E. Solid-state molecular nanomagnet inclusion into a magnetic metal–organic framework: Interplay of the magnetic properties. *Chem. Eur. J.* **2016**, *22*, 539–545. [[CrossRef](#)]
153. Graham, M.J.; Zadrozny, J.M.; Fataftah, M.S.; Freedman, D.E. Forging solid-state qubit design principles in a molecular furnace. *Chem. Mater.* **2017**, *29*, 1885–1897. [[CrossRef](#)]
154. Yaghi, O.M.; O’Keeffe, M.; Eddaoudi, M.; Chae, K.; Kim, J.; Ockwing, N.W. Reticular synthesis and the design of new materials. *Nature* **2003**, *423*, 705–714. [[CrossRef](#)]
155. Long, J.R.; Yaghi, O.M. The pervasive chemistry of metal–organic frameworks. *Chem. Soc. Rev.* **2009**, *38*, 1213–1214. [[CrossRef](#)]
156. Castellano, M.; Ferrando-Soria, J.; Moliner, N.; Cano, J.; Julve, M.; Lloret, F. Growth of thin films of single-chain magnets on functionalized silicon surfaces. *J. Coord. Chem.* **2018**, *71*, 725–736. [[CrossRef](#)]
157. Castellano, M.; Moliner, N.; Cano, J.; Lloret, F. Magnetic phase transition and magnetic bistability in oxamato-based Co^{II}Cu^{II} bimetallic MOF thin films. *Polyhedron* **2019**, *170*, 7–11. [[CrossRef](#)]
158. Geng, K.; He, T.; Liu, R.; Dalapati, S.; Tan, K.T.; Li, Z.; Tao, S.; Gong, Y.; Jiang, Q.; Jiang, D. Covalent organic frameworks: Design, synthesis, and functions. *Chem. Rev.* **2020**, *120*, 8814–8933. [[CrossRef](#)] [[PubMed](#)]
159. Dong, J.; Han, X.; Liu, Y.; Li, H.; Cui, Y. Metal–Covalent Organic Frameworks (MCOFs): A bridge between metal–organic frameworks and covalent organic frameworks. *Angew. Chem. Int. Ed.* **2020**, *59*, 13722–13733. [[CrossRef](#)] [[PubMed](#)]
160. August, D.P.; Dryfe, R.A.W.; Haigh, S.J.; Kent, P.R.C.; Leigh, D.A.; Lemonnier, J.-F.; Li, Z.; Muryn, C.A.; Leoni, I.; Song, Y.; et al. Self-assembly of a layered two-dimensional molecularly woven fabric. *Nature* **2020**, *588*, 429–435. [[CrossRef](#)]
161. Zao, Y.; Guo, L.; Gándara, F.; Ma, Y.; Liu, Z.; Zhu, C.; Lyu, H.; Trickett, C.A.; Kasputin, E.A.; Terasaki, O.; et al. A synthetic route for crystals of woven structures, uniform nanocrystals, and thin films of imine covalent organic frameworks. *J. Am. Chem. Soc.* **2017**, *139*, 13166–13172. [[CrossRef](#)] [[PubMed](#)]

Disclaimer/Publisher’s Note: The statements, opinions and data contained in all publications are solely those of the individual author(s) and contributor(s) and not of MDPI and/or the editor(s). MDPI and/or the editor(s) disclaim responsibility for any injury to people or property resulting from any ideas, methods, instructions or products referred to in the content.